OAK RIDGE
NATIONAL LABORATORY
MANAGED BY UT-BATTELLE
FOR THE DEPARTMENT OF ENERGY

ORNL/TM-2003/65

Reactor Physics Studies of Reduced-Tantalum-Content Control and Safety Elements for the High Flux Isotope Reactor

November 2003

R. T. Primm III

UT-BATTELLE
ORNL-27 (4-00)

ORNL/TM-2003/65

REACTOR PHYSICS STUDIES OF REDUCED-TANTALUM-CONTENT CONTROL AND SAFETY ELEMENTS FOR THE HIGH FLUX ISOTOPE REACTOR

R. T. Primm III

December 2003

Prepared by
OAK RIDGE NATIONAL LABORATORY
P.O. Box 2008
Oak Ridge, Tennessee 37831-6285
managed by
UT-BATTELLE, LLC
for the
U.S. DEPARTMENT OF ENERGY
under contract DE-AC05-00OR22725

CONTENTS

Page

LIST OF FIGURES

LIST OF TABLES

ACKNOWLEDGMENTS

The author would like to acknowledge the helpful and informative technical reviews of this document that were performed by J. C. Gehin and B. F. Siefken, both of Oak Ridge National Laboratory (ORNL), and by R. B. Rothrock, retired from ORNL. The author would also like to acknowledge the careful and prompt editing of C. C. Southmayd and the document preparation performed by M. L. Wells and B. J. Smith, all of ORNL. Finally, the author wishes to thank and acknowledge B. J. Marshall, Knolls Atomic Power Laboratory, and L. F. Miller, University of Tennessee, for their explanations and assistance in understanding prior studies performed on this topic.

EXECUTIVE SUMMARY

Some of the unirradiated High Flux Isotope Reactor (HFIR) control elements discharged during the late 1990s were observed to have cladding damage. The damage was limited to the tantalum/europium interface of the element and was thought to have resulted from interaction of hydrogen and europium to form a compound of lower density than europium oxide, thus leading to a "blistering" of the control plate cladding. Reducing the tantalum loading in the control plates should help preclude this phenomena.

The tantalum content in the regulating and safety elements for the HFIR will be reduced from the current value of 38 vol % to 30 vol %. To perform a safety assessment of this reduction, selected computer programs and data libraries were validated. While there is not perfect agreement among calculated and measured power distributions, the studies enable quantification of changes in the reactor core power distribution due to the changes in the safety and regulating elements. Calculations indicate essentially no changes in the power distributions due to the proposed reduction in tantalum content. The calculated differential control element worths at critical configurations for the reduced tantalum elements as compared to existing elements were determined to be unchanged within the accuracy of the computational method and relevant experimental measurements. Differential safety element worth values for the reduced-tantalum-content elements are reported for postulated accident conditions and are shown to be greater than values currently assumed in HFIR safety analyses.

The studies of reactor power distribution and differential rod worth confirm that the proposed reduction in tantalum content would not increase the consequences of an accident previously evaluated in the safety analysis. Because the differential worth of the reduced tantalum elements is the same as for existing elements at critical configurations, the reduction in tantalum content would not increase the consequences of a malfunction of equipment important to safety previously evaluated in the safety analyses. Since no changes are being made in element geometry, choice of constituent materials, or control circuitry, the proposed reduction in tantalum content would not create the possibility of a malfunction of equipment important to safety of a different type other than any previously evaluated in the safety analyses.

The Research Reactors Division procedure for estimating the symmetric critical control element position will have to be revised prior to the insertion into the reactor of the reduced tantalum control and safety elements. Other than noting the composition of the new control and safety elements, no revisions are required to either the technical safety requirements or the safety analysis report for the HFIR.

REACTOR PHYSICS STUDIES OF REDUCED-TANTALUM-CONTENT CONTROL AND SAFETY ELEMENTS FOR THE HIGH FLUX ISOTOPE REACTOR

R. T. Primm III

ABSTRACT

Some of the unirradiated High Flux Isotope Reactor (HFIR) control elements discharged during the late 1990s were observed to have cladding damage—local swelling or blistering. The cladding damage was limited to the tantalum/europium interface of the element and is thought to result from interaction of hydrogen and europium to form a compound of lower density than europium oxide, thus leading to a "blistering" of the control plate cladding. Reducing the tantalum loading in the control plates should help preclude this phenomena. The impact of the change to the control plates on the operation of the reactor was assessed.

Regarding nominal, steady-state reactor operation, the impact of the change in the power distribution in the core due to reduced tantalum content was calculated and found to be insignificant. The magnitude and impact of the change in differential control element worth was calculated, and the differential worths of reduced tantalum elements vs the current elements from equivalent-burnup *critical* configurations were determined to be unchanged within the accuracy of the computational method and relevant experimental measurements. The location of the critical control elements symmetric positions for reduced tantalum elements was found to be 1/3 in. less withdrawn relative to existing control elements regardless of the value of fuel cycle burnup (time in the fuel cycle). The magnitude and impact of the change in the shutdown margin (integral rod worth) was assessed and found to be unchanged. Differential safety element worth values for the reduced-tantalum-content elements were calculated for postulated accident conditions and were found to be greater than values currently assumed in HFIR safety analyses.

1. INTRODUCTION

The High Flux Isotope Reactor (HFIR) is composed of two, concentric annuli of highly enriched uranium (HEU) fuel, surrounded radially by a beryllium reflector. The regulating and safety elements for the reactor are located in an annulus between the HFIR core and reflector and contain three regions: a "black" strong neutron-absorber region containing Eu_2O_3 dispersed in an aluminum matrix; a "gray" moderate neutron-absorber region with tantalum particles in an aluminum matrix; and a "white" region (or follower) of perforated aluminum. Figure 1 is a schematic of the HFIR regulating and safety elements.

The last set of unirradiated regulating or safety elements was loaded into the HFIR in the fall of 2002. All of the current inventory of irradiated elements (still usable) were expected to achieve the end of their useful life by 2006.

During fiscal year (FY) 2003, a fabrication process for new elements will be initiated. J. D. Sease, Oak Ridge National Laboratory (ORNL), notes that approximately 32 "quarter plates" will be fabricated. Each shim/regulating cylinder is composed of four plates welded together. In a "safety element," the four plates can move individually (four independent drive systems); though in normal operation, the plates are "ganged," and movements are coordinated (same axial positions).

The design goal for the 2003 control element fabrication process is to manufacture at least three shim/regulating cylinders that meet or exceed all specifications. With the corresponding three sets of four

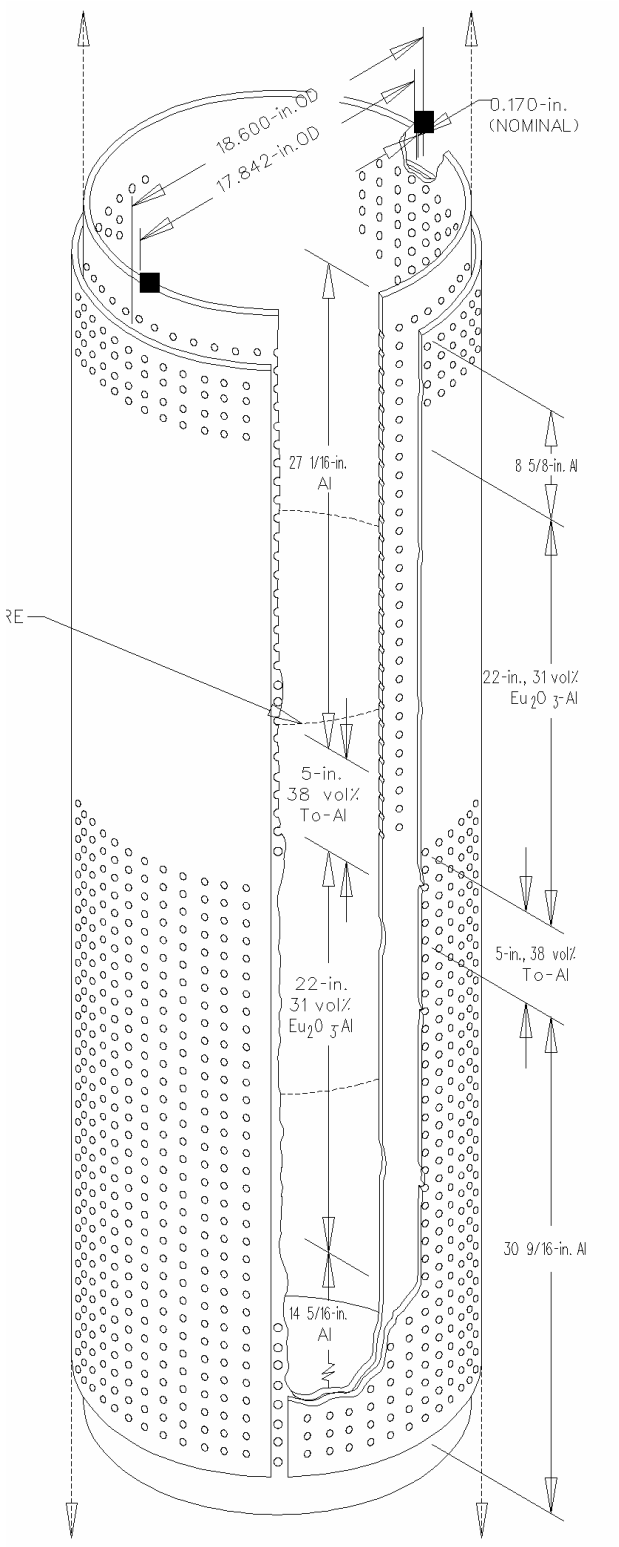

Fig. 1. HFIR regulating and safety elements.

safety blades, the "milestone" for the project is that 24 of the 32 plates must meet acceptance criteria. As with most manufacturing processes, the largest increment of cost is associated with the production of the first-of-a-kind. Sease estimates the cost of the first plate, that is, the cost of all preparatory studies and establishment of a production line, to be about $2,000,000 with the cost of each subsequent plate being $100,000 to $200,000. The total cost of this project is approximately $7,000,000, and the time to complete the fabrication project is estimated to be 3–4 years.*

Some of the unirradiated HFIR control elements stored in the HFIR pool during the late 1990s were observed to have cladding damage—local swelling or blistering (see Fig. 2). The cladding damage was limited to the tantalum/europium interface of the element and is thought to result from interaction of hydrogen and europium to form a compound of lower density than europium oxide, thus leading to a "blistering" of the control plate cladding. The elements were rendered unusable.

The blistering is thought due to free hydrogen from the reactor coolant that can enter the tantalum zone via the holes punched in the control plates, the holes being present to equalize the pressure on both sides of the plate (see Fig. 1). If a continuous pathway of tantalum metal exists from a hole to the europium/tantalum interface, the hydrogen can migrate along this path until it reaches the europium/tantalum interface and bonds with the europium. Tantalum volume percentages of slightly greater than 38% can lead to the presence of continuous tantalum metal "streamers" in the tantalum zone during the fabrication process for the control element (rolling of the tantalum/aluminum billet to create a plate).

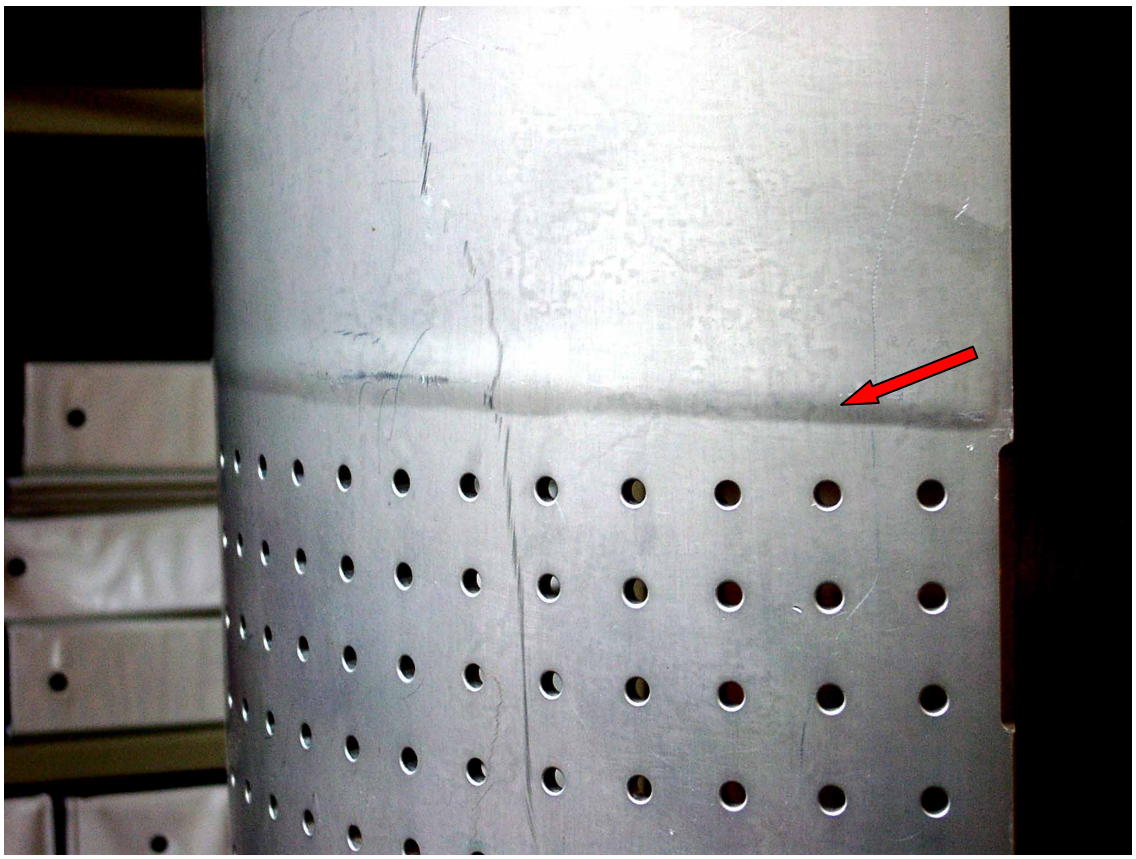

Fig. 2. Blister at tantalum/europium interface.

*It is currently planned that the plates would be manufactured at ORNL due to the requirement for strict manufacturing tolerances and due to the lack of commercial market for the product; HFIR would be the "single user" in the United States.

Reducing the tantalum content from its current value should help alleviate the control element degradation by ensuring that the tantalum remains as a discrete powder, not forming the continuous metal pathway to the europium region.

Sease and other materials experts at HFIR think that the chemical "damage mechanism" (hydrogen migration from the perforations to the europium region) likely would be aggravated by increased temperatures relative to nominal operating conditions. Decays of tantalum isotopes 182 and 183 are the major heat sources in the control elements. After reactor shutdown and subsequent establishment of natural circulation, the temperatures in the control and safety elements are at their highest values. Though this mechanism could not have caused the failure shown in Fig. 2 (that element was not irradiated), reducing the tantalum content of the elements would obviously reduce this heat source and might mitigate the production of a blister on an element during or following irradiation.

"Scoping" studies were conducted to determine the impact on reactor physics parameters of reducing the tantalum content of the regulating/safety elements. Based on studies documented in ref. 1, it was concluded that the tantalum content in the regulating and safety elements could be reduced from the current value of 38 vol % to 30 vol % but that "further reductions … may prove problematic."

During FYs 2001 and 2002, R. B. Rothrock, ORNL, attempted to determine if such a change in the tantalum content would constitute an unreviewed safety question. The conclusion of his studies was that computational analyses were needed to assess whether such a change in regulating and safety element composition was bounded by existing safety margins. This conclusion was reached because modification of the tantalum content of the regulating and safety elements would be the first significant change to the nuclear design of the HFIR regulating/safety elements since the reactor began operation (mid-1960s).

Specifically, Rothrock determined that physics calculations were needed to answer three questions.

1. Could the proposed activity increase the consequences of an accident previously evaluated in the safety analysis?
2. Could the proposed activity increase the consequences of a malfunction of equipment important to safety previously evaluated in the safety analyses?
3. Does the proposed activity create the possibility of a malfunction of equipment important to safety of a different type other than any previously evaluated in the safety analyses?

Rothrock identified a need to perform two sets of calculations (all using the same computer models, software, and nuclear data). Relating to nominal, steady-state reactor operation, the impact of the change in the *power distribution* in the core due to reduced tantalum content had to be calculated. Relating to transient operation, the magnitude and impact of the change in differential control element worth (*scram reactivity insertion rate*) had to be calculated and assessed. Because the shutdown margin (integral rod worth) is determined by the europium content of the elements and this is to remain unchanged, no change in shutdown margin would result from a reduction in tantalum. Implicit in these studies was the determination of the points-in-time in a fuel cycle and in the lifetime of the control elements at which the impact of the change in tantalum concentration was the greatest. It is a goal of this report to provide documentation of these calculations.

While it will be shown that there is not perfect agreement among calculated and measured power distributions, the studies enable the author to quantify changes in the power distributions. It will be shown that all of the calculational results indicate essentially no changes in the power distributions due to the proposed reduction in tantalum content. Differential control element worth values for the reduced-tantalum-content elements will be reported and will be shown to yield integral element worths for postulated accident conditions that are greater than values currently assumed in HFIR safety analyses.

2. METHOD OF ANALYSIS

The reactor physics basis for the current safety margins for the operation of the HFIR is ref. 2. That report contains data for a series of critical experiments conducted in the HFIR (designated HFIRCE-4 in the report, but conducted with fuel elements designated as HFIRCE-3*). Power distributions and regulating and safety element worths were measured for a variety of regulating/safety element positions. Soluble boron in the water in the coolant channels of the fuel elements was used to simulate reactivity loss due to burnup. Calculated reactor physics parameters, validated with these measurements, are the reactor physics input to the safety basis for the current regulating/safety element design (38 vol % tantalum).

The operating power for the HFIR (ignoring vessel fluence considerations) is determined by the "hot spot" and "hot streak" factors.† The hot streak is defined to be the radial location in the core at which the axially integrated linear power density has the highest value. It is at this location that the local coolant exit temperature is highest. The thermal limits for the operation of the core are to avoid "burnout" heat flux at any location and avoid flow instabilities (when that criterion is more restrictive) in adjacent channels.

It is theoretically possible that a local region at a radial location different from the hot streak might have a power density higher than that found at any axial location along the hot streak. Thus, while the coolant flow exiting at that radial location might be subboiling, some degree of boiling could, in theory, occur at the local hot spot. To ensure that the current HFIR steady-state thermal-hydraulic analysis remains valid when the tantalum content of the control elements is reduced to 30%, it is necessary to examine the changes that occur in the hot spot and hot streak factors due to the modification in the tantalum content.

The safety basis thermal-hydraulic analyses use values for hot spot and "hot channel" (or hot streak) factors from computations validated with experiments. Differential regulating and safety element reactivity functions were determined from experimental measurements. Because there are no measured values for a system containing 30 vol % tantalum control elements, the safety basis for those elements will be based on the calculations reported in this document.

Three of the critical experiments documented in ref. 2 were selected to validate nuclear analysis computer codes and data. These configurations are shown in Figs. 3–5 and are reprints of Figs. 7.8, 7.5, and 7.6, respectively, of ref. 2. Control element position as a function of burnup for four HFIR fuel cycles is shown in Fig. 6 (ref. 3). The regulating/safety element positions in the critical experiments depicted in Figs. 3–5 correspond to beginning-, middle-, and near-end-of-cycle (EOC) configurations. (Actual EOC conditions were not examined because the power distribution would be generally independent of the tantalum concentration since the poison regions of the elements are fully withdrawn from the fueled region of the core.)

---

*The HFIRCE-3 fuel element was constructed differently from the production HFIR cores so that various reactor physics measurements could be conducted. The two parts (inner and outer element) were fastened together and loaded into the reactor at the same time, and they were contained within a can (i.e. the outer element envelope was water-tight). The dry assembly was loaded into the reactor with the reactor water level lowered below the bottom of the fuel. The fuel assembly was then filled to the top of the assembly with a hose and pump. As a consequence, the borated water was contained in the fuel element coolant channels and upper and lower plenum of the fuel element. The remainder of the reactor (including control region water gaps) was filled with ordinary demineralized water. This configuration mimics the configuration in the critical facility, which was also performed with the CE-3 element. Furthermore, this configuration avoided having to deborate all the water in the plant. At the completion of these experiments, the inner and outer elements of the CE-3 were separated and stored at the Oak Ridge Y-12 Plant.

†In this report, the terms "hot spot" and "hot track or streak" are interpreted in terms of nuclear heat production. In many HFIR-related thermal-hydraulic reports, these terms generally refer to hypothetical locations (spots or tracks) in the core where the worst combination of tolerances combines with the nominal power distribution to result in the closest approach to thermal limits. The hot spot/streak factors usually are taken to be multiplicative factors based on engineering uncertainties or fuel assembly tolerances, which are multiplied into the nominal nuclear power density (or flow, etc,) to obtain the design values to be compared against thermal limit criteria. In general, the locations of highest nominal nuclear power density (i.e., at or near the core midplane) are not the ones where the thermal limit criteria are most closely approached; this is normally at the core outlet.

Computational models, data, and procedures for the HFIR experiments are described in ref. 1. These models were modified to correct deficiencies also identified in ref. 1. All calculations were performed with the SCALE 4.4a and DOORS 3.2 computational packages available from the Radiation Safety Information Computational Center and installed on UNIX alpha workstation ossws5.ornl.gov in compliance with applicable Research Reactors Division (RRD) procedures.

Following validation, the same critical experiment configurations were calculated under the assumption that the tantalum content in the regulating and safety elements had been reduced by 21% (from 38 wt % to 30 wt %). Multiplication factors and power distributions were determined. Changes in the hot spot and hot streak locations and magnitudes were then tabulated and compared to available safety margins. Additional calculations were performed to determine the reduced-tantalum-content regulating and safety element positions that yielded the same multiplication factor as for the reference critical experiments. From these calculations, differential rod worths for beginning-, middle-, and near-end-of-life (EOL) conditions for the reduced-tantalum-content elements were calculated and compared to values for the 38 wt % tantalum content control elements—the current differential rod worth curve being derived from the critical experiments being reanalyzed here.

2.1 COMPUTATIONAL METHODS AND DATA

Representative datasets are provided in Appendix A and are based on models presented in ref. 1. All calculations are performed with 44 energy group, ENDF/B-V cross sections derived from the SCALE 238 group, ENDF/B-V library (ref. 4). For all eigenvalue calculations, k-effective values are converged to 10^{-5} or tighter, and the fission source was also converged to 10^{-5} or tighter. (One cent in reactivity for the HFIR core corresponds to a change in k-effective of about 7.6×10^{-5}.) The convention is used in this document that calculated parameters are reported to the number of significant digits such that the convergence in the value of the number is less than or equal to a unit deviation in the last digit. For example, a calculated k-effective value of 0.991253 would be the result from a calculation in which the k-convergence is less than or equal to 0.000001.

AMPX modules accessed via the SCALE4.4a system were used to perform resonance processing (BONAMI and NITAWL), and one-dimensional, discrete ordinates transport theory (XSDRNPM) calculations were performed to spatial and energy weight the cross section data from 238 to 44 groups (SCALE 44 group structure). Utility modules (ALPO in SCALE and GIP in DOORS) were used to convert cross section data to ANISN format for use in the DORT eigenvalue calculation. Additional information regarding these steps was documented in ref. 1.

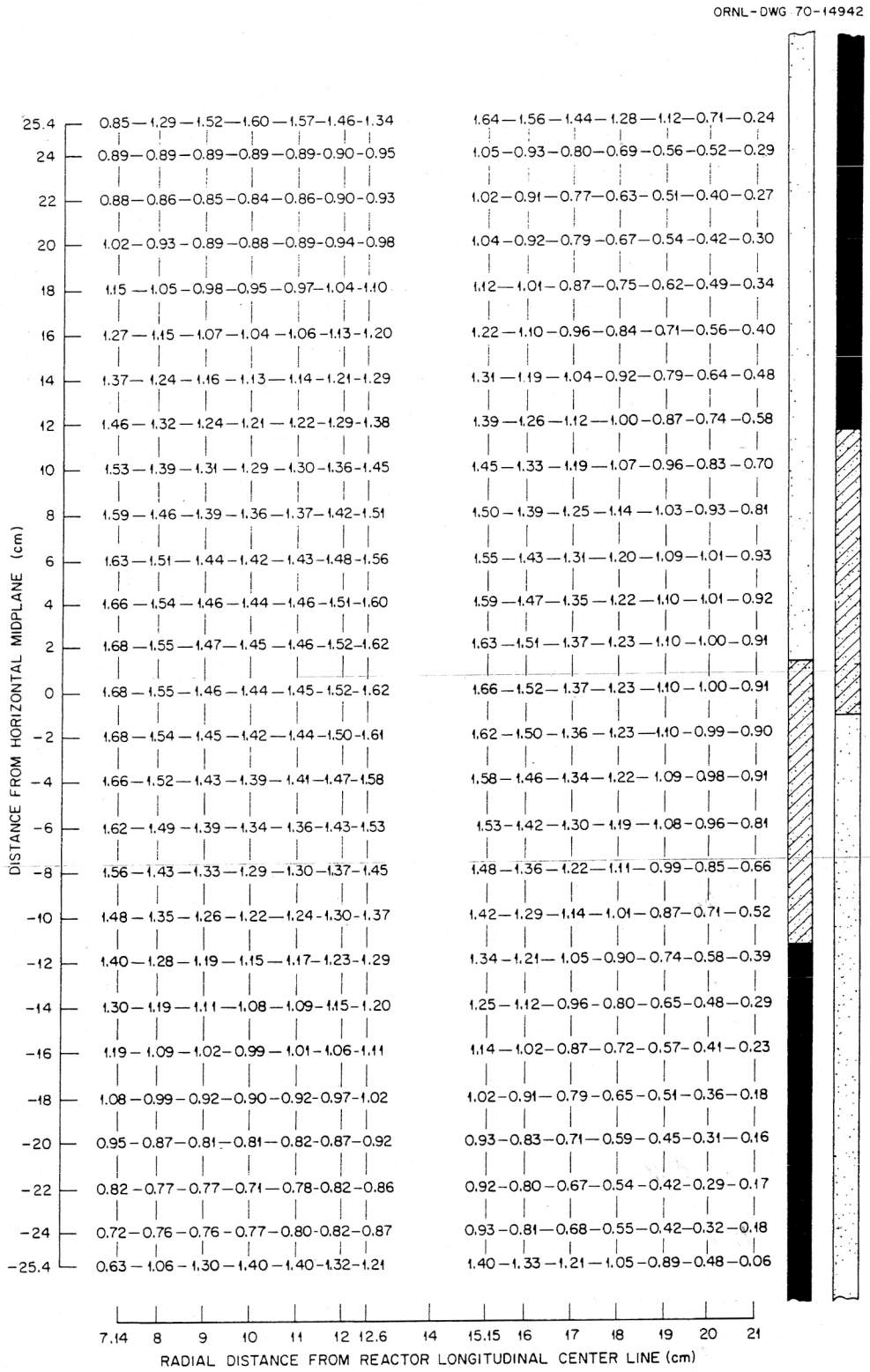

Fig. 3. Critical experiment, simulated beginning-of-life (BOL) regulating/safety element positions—16.6 in. withdrawn.

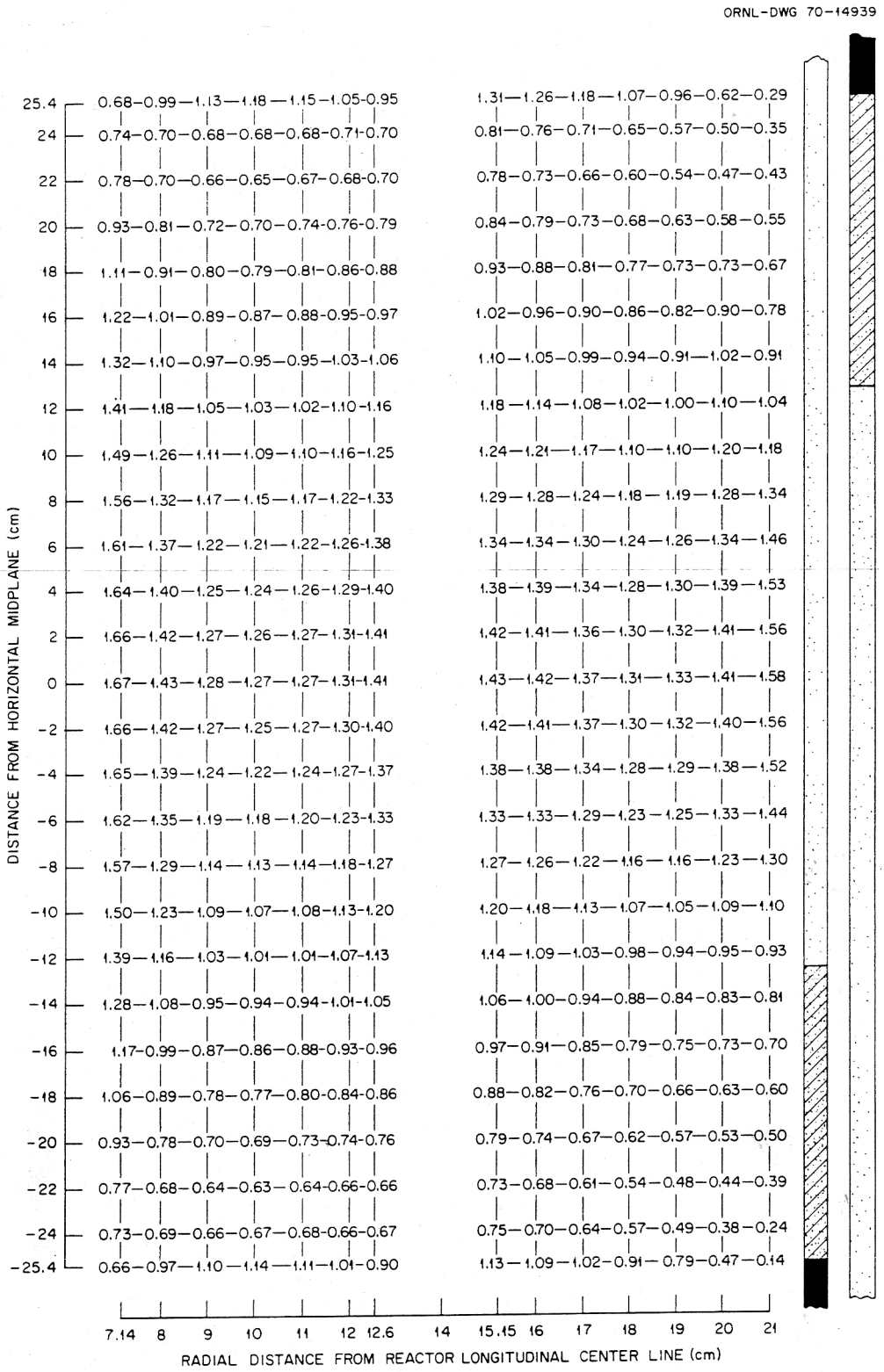

Fig. 4. Critical experiment, near-middle-of-life regulating/safety element positions—21.295 in. withdrawn.

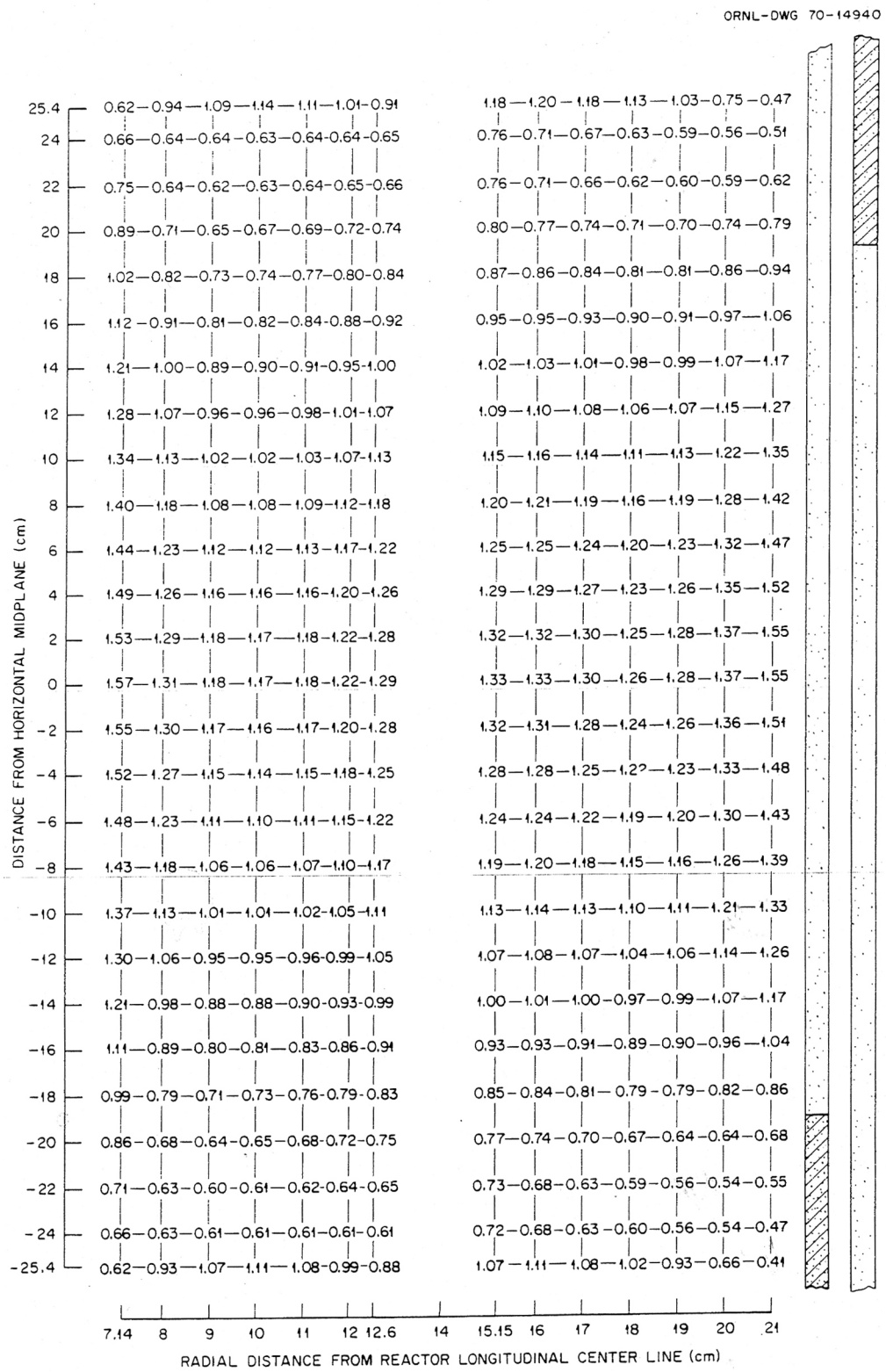

Fig. 5. Critical experiment, near-end-of-life (EOL) regulating/safety element positions—24.3 in. withdrawn.

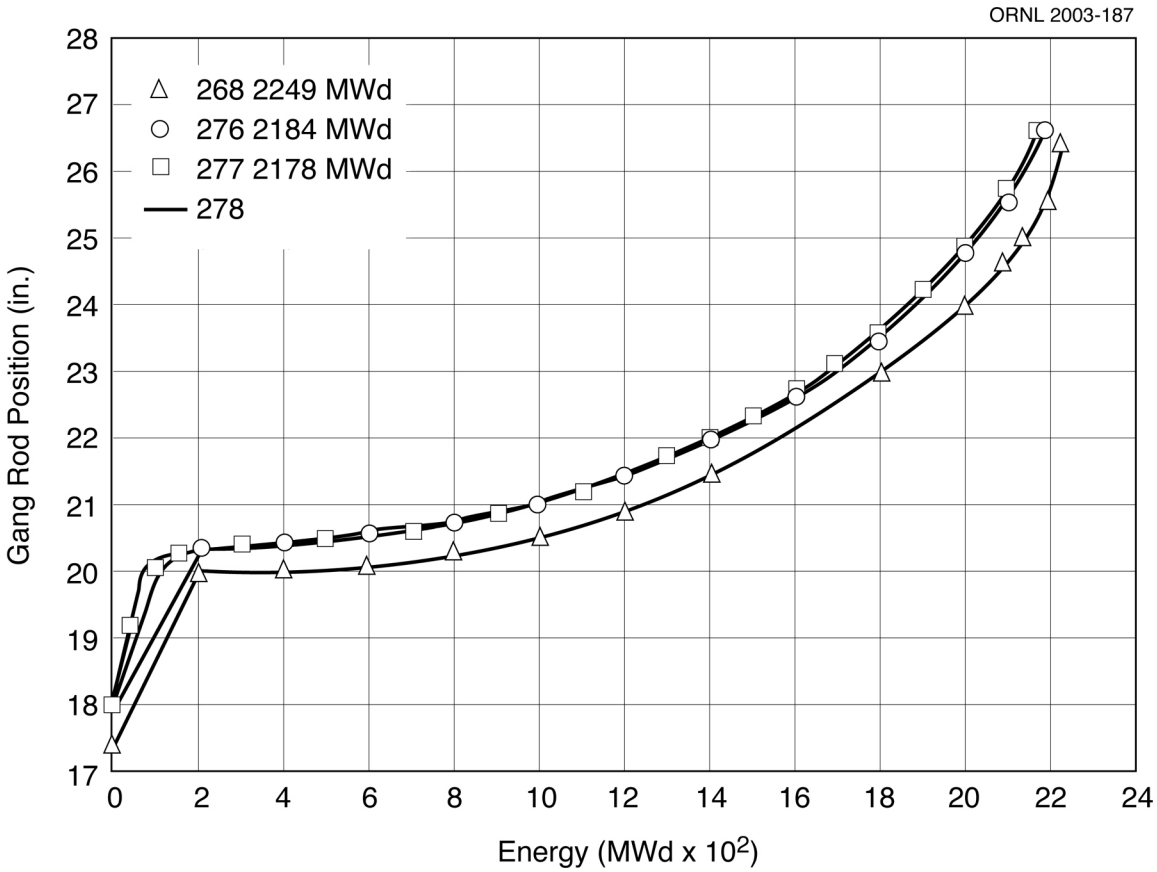

Fig. 6. Regulating/safety element positions for four fuel cycles.

A significant modification from the reactor model (DORT) described in ref. 1 was the refinement of the model to explicitly include the coolant gaps and poison regions of the control annular region. The geometric model described in Appendix A of ref. 2 homogenizes these regions into two zones. In ref. 2, the fuel element side plate, water, clad, and interior portion of the control element (either Eu, Ta, or Al) were homogenized into one zone. Likewise, the corresponding regions of the safety plate were homogenized. For the work presented here, discrete representation of these regions, described in Appendix B, was performed with the intent of improving the accuracy of the calculation.

2.2 RECENT VALIDATION STUDIES

Three studies have been performed with methods and data similar or the same as those used in this study. All three made use of the AMPX/SCALE cross section processing system, and all used cross section data derived from the ENDF/B-V data files.

Validation studies using the diffusion theory-based computer program, VENTURE,* are reported in refs. 3, 5, and 6. Reference 3 provides a comparison of calculations to the derived-from-measurement power distributions that are presented subsequently in this report. References 5 and 6 describe the same set of calculations and provide calculation-to-experiment comparisons at the foil irradiation locations described in Appendix A of ref. 2 (rather than the distributions derived from those foil irradiations that are

*Original reference is D. R. Vondy, T. B. Fowler, and G. W. Cunningham III, *The Bold Venture Computation System for Nuclear Reactor Core Analysis, Version III*, ORNL-5711, June 1981. The software package, along with additional documentation, is now available from the Radiation Safety Information Computational Center, Oak Ridge National Laboratory as package CCC-654, titled VENTURE-PC 1.1.

also presented in ref. 2 and previously in this report). The work in ref. 6 considers only the beginning-of-life (BOL) critical configuration described subsequently. Both sets of calculations use fewer energy groups than the current work (7 and 11 for refs. 3 and 6, respectively). Neither differential nor integral control element worth is calculated in these studies.

A validation study using the DORT computer program was performed and documented in ref. 7. Only the BOL critical configuration was considered. The calculation was performed with 39 energy groups. Fluxes at various locations were reported, but the calculated value of k-effective was not reported. However various reactivity coefficients were compared to measured values from ref. 2, and agreement was good. Differential or integral control element worths were not calculated.

2.3 METHODS DEVELOPMENT

During the conduct of these studies, the need for development or research was identified in several areas. While not needed for the successful accomplishment of these studies, these needs are identified in Appendix C so that they may be included in the long-range planning process for the HFIR.

3. IMPACT OF TANTALUM CHANGE ON NOMINAL, STEADY-STATE OPERATION

3.1 SIMULATED BEGINNING-OF-LIFE CONDITION

3.1.1 Validation with Existing Regulating/Safety Element Configuration

Using the computational scheme described in Sect. 2, the values of k-effective (effective multiplication factor) and various local power densities were computed for the critical experiment pictured in Fig. 3. The calculated k-effective for the *critical* (k-effective experimental = 1.0) was 0.980045. While the level of agreement between calculation and experiment was less than desired, it was better than that obtained by the authors of ref. 2 (see caption to Fig. 7.14, k = 0.96).

The *level of agreement* between calculated and measured local power density distribution is shown in Fig. 7. (The actual power density distribution is that provided in Fig. 3.) Reference 2 notes (pg. 92) that "the overall accuracy of the overall (measured) power distribution was about ±5% (97% of the points agree within ±5%)." In fact, variations of more than 5% can be expected because neither Fig. 3, 4, nor 5 yield a relative core power density of 1.0 when the reported measured values are integrated over the volumes defined by equal distances between mesh points at which the values are reported. The discrepancies are small, between 1–2% and positive (integrated, reported, measured values are all high). Areas of concern, then, would be those positions in which the deviation between calculated and experimental exceeds 7%. As is seen in calculations reported in ref. 2, the locations of the points with greatest discrepancy are at the edges—both radial and axial—of the fuel elements.

Tables 1 and 2 show the measured and calculated streak factors. Data from these tables are plotted in Fig. 8. The radial locations for which streak factors are reported differ because of choices made during the measurements (derivation of local power densities from measured foil activations) and analyses (choice of mesh point location) reported in ref. 2.

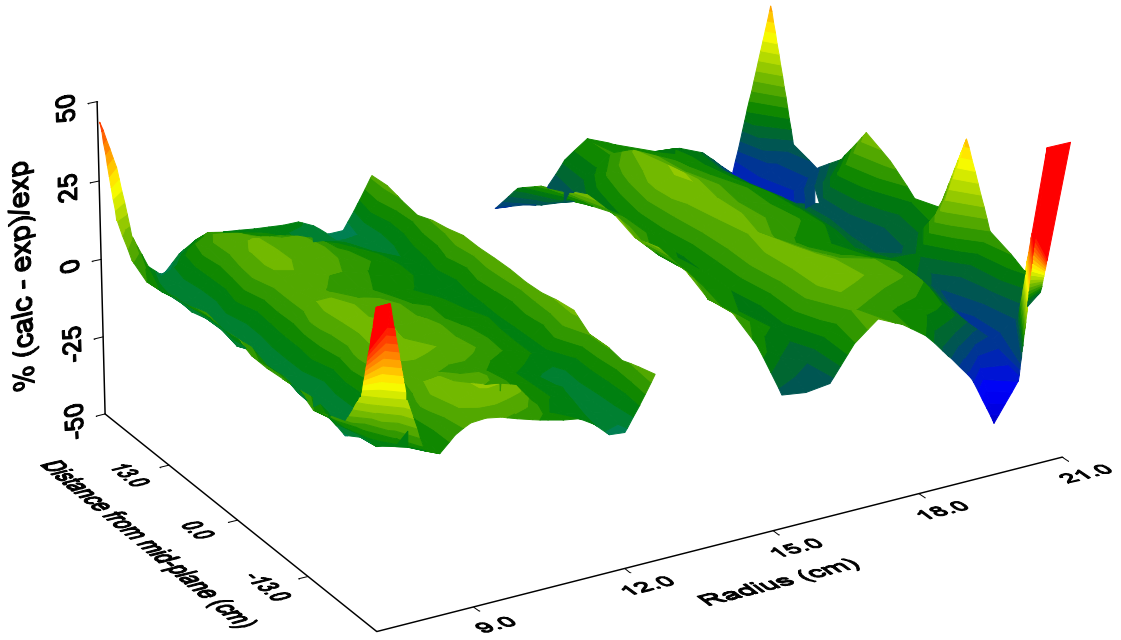

Fig. 7. Level of agreement between calculated and measured local power densities at BOL conditions.

Table 1. Measured streak factors from Fig. 3 (simulated BOL)

Radius (cm)	Relative streak factor
7.14	1.3171
8.0	1.2287
9.0	1.1696
10.0	1.1469
11.0	1.1632
12.0	1.2142
12.6	1.2807
15.15	1.3136
16.0	1.1955
17.0	1.0595
18.0	0.9317
19.0	0.8020
20.0	0.6706
21.0	0.5212

Table 2. Calculated streak factors for Fig. 3

Radius	Relative streak factor
7.320	1.295
7.750	1.246
8.250	1.207
9.000	1.173
10.000	1.170
11.000	1.176
11.750	1.195
12.300	1.252
15.325	1.292
15.750	1.234
16.250	1.183
17.000	1.089
18.000	0.941
19.000	0.793
19.750	0.678
20.250	0.600
20.750	0.537

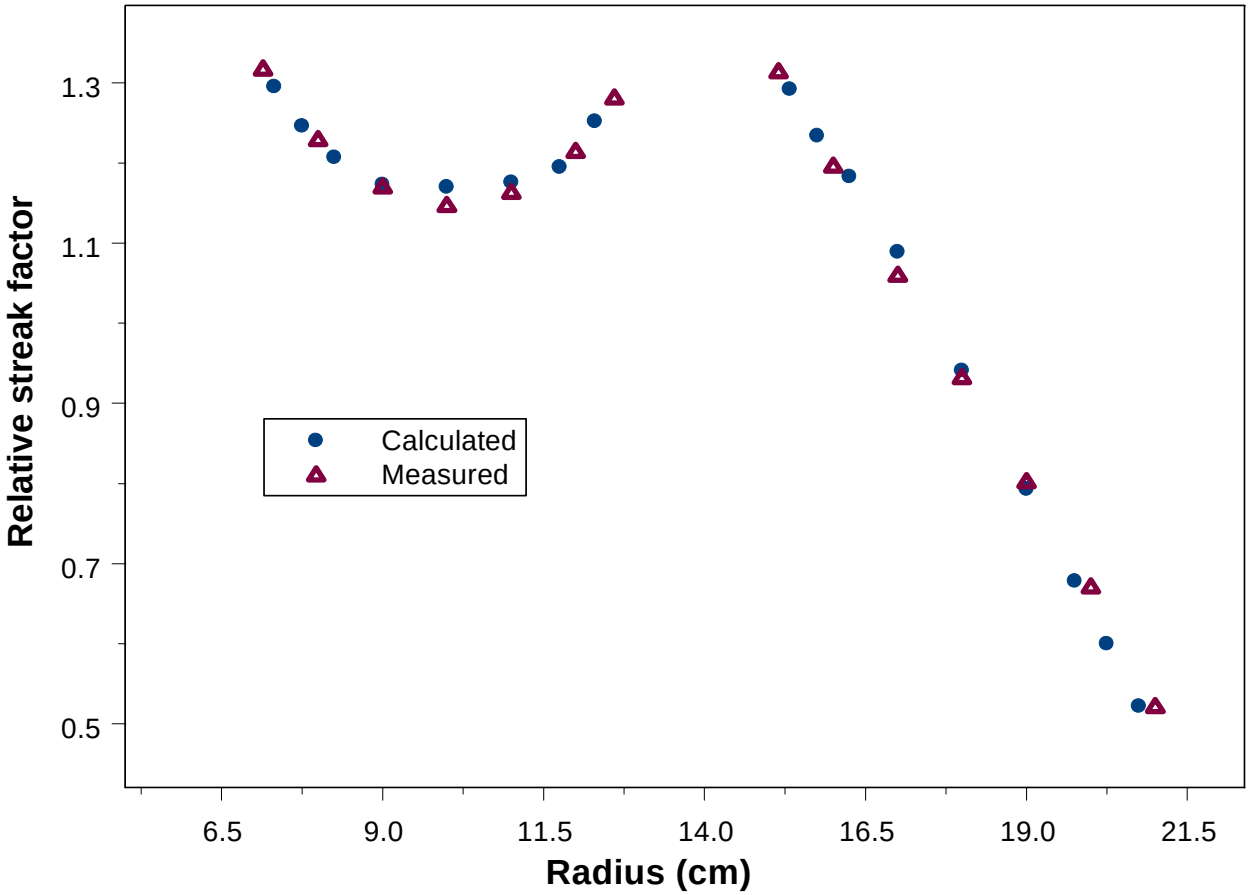

Fig. 8. Comparison of measured and calculated streak factors.

The agreement between measured and calculated streak factors is excellent. While the calculated hot streak is at the same location as the measured hot streak, the differences between the streak values for the inside edges of the inner and outer elements are significantly less than the reported uncertainties in the measurements. The comparison in Fig. 8 indicates that the ability to calculate the magnitude and location of the hot streak factor at BOL is excellent.

The location and magnitude of the measured hot spot (from Fig. 3) is 1.68 at three points along the inside edge of the inner element (radius = 7.14 cm, axial heights of +2, 0, and –2). The calculated values of the relative local power density at those three locations are 1.803, 1.807, and 1.792, respectively. The two sets of data agree to 7–8%, but more important is the fact that the computational mesh is finer than the measurement mesh. When the location being examined is at any of the edges of the fuel elements, the finer computational mesh can lead to a larger local value than in the larger, measured mesh. One could compensate by appropriately integrating/subdividing the computational mesh to match the measured mesh, but the effort is deemed superfluous.

The location and magnitude of the calculated hot spot was 1.822 at a radius of 15.21 and axial location of 1.01 (axial middle of the inside edge of the outer element). The corresponding measured value at that location was 1.64 (average of values at z = 0 and 2). This discrepancy of 11% was greater than expected from experimental uncertainty but was conservative.

These comparisons indicate that the ability to calculate the hot spot location and magnitude is less than that of the hot streak factor. However, the discrepancy is conservative.

3.1.2 Reduced-Tantalum-Content Regulating/Safety Elements

3.1.2.1 Calculated physics parameters for configuration critical with existing regulating/safety element design

The reactor model used for the calculations reported in Sect. 3.1.1 (Fig. 3 configuration) was modified to reduce the tantalum content of both the regulating and safety elements from 38 vol % to 30 vol %. The location of the elements was unchanged. Obviously, if such a configuration was created in the reactor, the system would be supercritical. The calculation was performed to determine the relative worth, at BOL, of the tantalum modification and compare the value to the differential worth of the existing regulating/safety elements.

The calculated k-effective was 0.987170. Assuming an effective delayed neutron fraction for the HFIR fuel of 0.0076 (the value noted in the HFIR USAR, Sect. 4.3.2.1), the change in reactivity from the 38 vol % tantalum case due to reducing the tantalum content was 94 cents.

The differential worth of the existing regulating/safety element combination with elements withdrawn to 42.1 cm (16.6 in.) is 309 cents/in. (see Fig. 9). The change in tantalum content corresponds to a joint regulating/safety insertion of about 1/3 in.—less than the deviation currently allowable under RRD procedure RTP-2 (procedure for estimating the startup position for HFIR regulating and safety elements).

The calculated hot streak factor for this configuration (1.283) was slightly less than the value for the 38 vol % control rod case and was located at the inside edge of the outer element. The location of the hot spot factor was unchanged and the magnitude was insignificantly less (1.807). Apparently the slight reduction in tantalum results in a slight, radially outward shift in the power distribution.

3.1.2.2 Expected beginning-of-cycle (BOC) configuration for reduced-tantalum-content regulating/safety elements

A study was conducted to determine the regulating/safety element withdrawal level that yielded a calculated k-effective equal to the value noted in Sect. 3.1.1 (the critical Fig. 3 configuration). An element withdrawal of 16.3 in. (41.4 cm) was found to yield a k-effective of 0.980463 (±0.000002), only 0.04% different from the "critical" value found for the existing regulating/safety element design (Sect. 3.1.1).

Local power densities for this new critical configuration were calculated and compared to the calculated local power densities for the existing regulating/safety element design (Sect. 3.1.1 calculations). The location of the hot streak factor was unchanged and the magnitude was insignificantly higher (1.294). The location and magnitude of the calculated hot spot were essentially unchanged (inner edge of outer element with a value of 1.826). The value of the relative local power density at the measured hot spot locations (inner element, heights of 2, 0, and −2) were 1.806, 1.808, 1.792—insignificantly different from the values calculated for the critical configuration of Fig. 3.

When comparing the critical configuration with 38 vol % tantalum to the critical configuration with 30 vol % tantalum, the values of the calculated relative local power densities at the inside edges of the inner and outer fuel elements at the base of the elements—outlets of the measured and calculated hot streaks—decreased but by an insignificant amount. For the inner element, inner edge, and outlet, the relative power density decreased from 1.135 to 1.131. For the outer element, inner edge, and outlet, the relative power density decreased from 1.293 to 1.287.

3.1.3 Differential Element Worth for BOC Conditions

The differential regulating and safety element worth values as a function of element position for the currently used elements are shown in Fig. 9. (Note that full insertion corresponds to 27 in. and that at full insertion, the europium/tantalum interfaces of the control and safety plates are at 2 in. above/below the

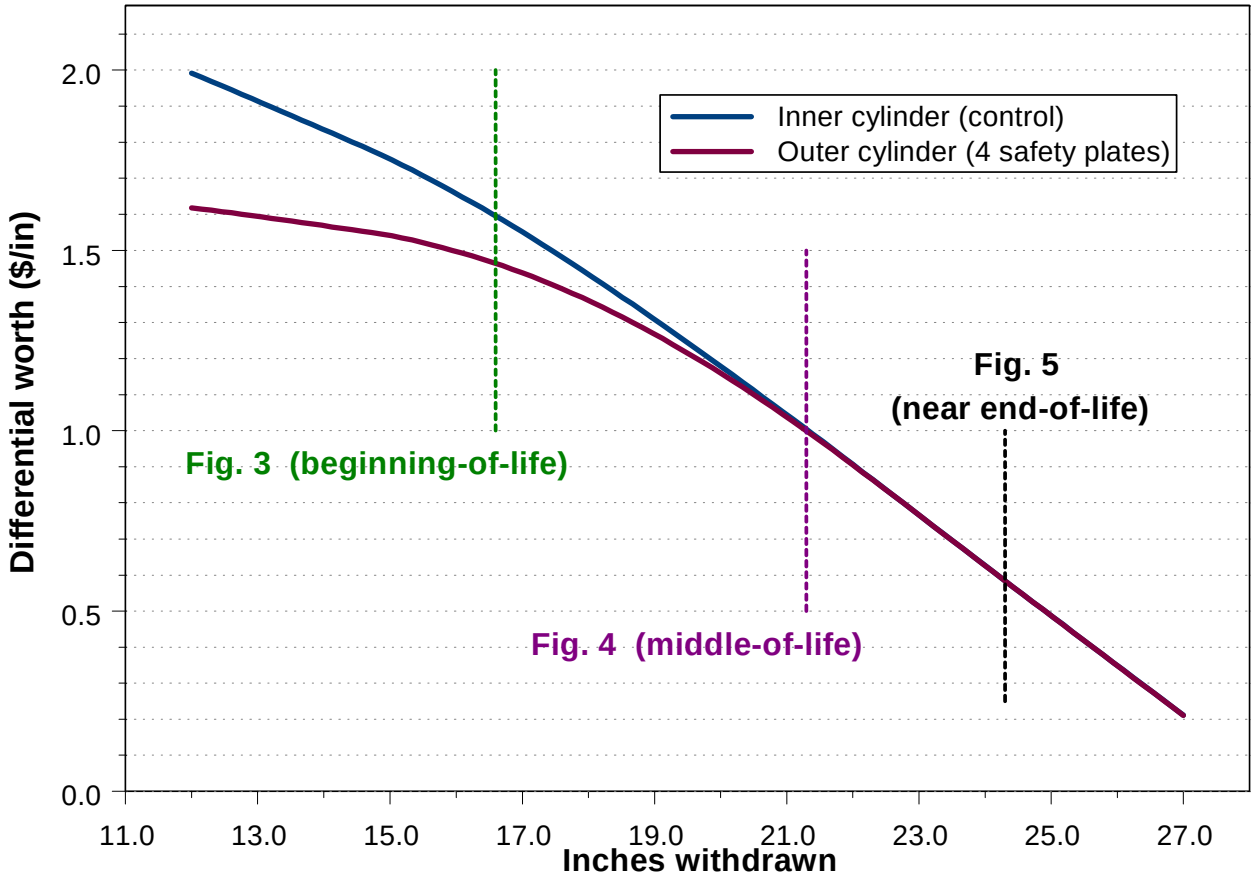

Fig. 9. Differential worth values for 38 vol % tantalum regulating and safety elements.

edges of the fueled regions of the core.) Figure 9 is based on experimental measurements (ref. 2 and ref. 8) in both the critical facility and in the HFIR. However, different data are currently the basis for reactor operations and also for safety analyses (ref. 9). Similar curves will be developed for reduced-tantalum-content regulating and safety elements. One of the HFIR procedures, RTP-2, *Procedure for Determining the Beginning of Cycle ESCCEP of HFIR Control Plates*, will have to be revised to incorporate the new reactivity worth values prior to the installation of reduced tantalum regulating/safety elements. Comments on this procedure are presented in Appendix D.

From Fig. 9, the differential element worth for the current regulating/safety elements at an element withdrawal of 16.6 in. (the value for Fig. 3), was 309 cents/in. The positions of the regulating and safety elements in the computational model for Fig. 3 (Sect. 3.1.1) were modified so that a differential worth value could be computed and compared to the measured data from Fig. 9. The calculated differential worth was 280 cents/in. (131 cents/in. for the four safety plates and 149 cents/in. for the regulating element).

The differential worth for the reduced-tantalum-content elements at their BOC configuration can be inferred from the multiplication factors computed in Sects. 3.1.2.1 and 3.1.2.2 but was recalculated with separate perturbations of the safety and regulating elements. The calculated worth was 293 cents/in. (138 cents/in. for the four safety plates and 155 cents/in. for the regulating element). The slightly larger value relative to the 38 vol % case (305 cents) might be due to the slightly greater insertion of the control elements for the reduced tantalum critical configuration [differential worth increases as amount of insertion increases, up to the point at which the tantalum/europium interfaces of the safety and regulating elements are aligned—15 in. of insertion, that is, 12 in. of withdrawal (see Fig. 9)].

3.1.4 Conclusions Regarding the Use of Reduced-Tantalum-Content Regulating/Safety Elements at BOC

The expected change in startup regulating/safety element withdrawal position for the reduced-tantalum-content elements vs the current design is –0.3 in. The magnitudes and locations of the hot streak and hot spot factors for a BOC critical configuration with the reduced tantalum regulating/safety elements are unchanged from the values for the BOC critical configuration with the existing regulating/safety elements. The differential regulating/safety element worth at the BOC critical configuration for the reduced tantalum elements is the same or slightly greater than the differential worth for the existing regulating/safety elements at the BOC critical configuration for those elements.

3.2 SIMULATED MIDDLE-OF-CYCLE CONDITION

3.2.1 Validation with Existing Regulating/Safety Element Configuration

The analyses discussed in Sect. 3.1 were repeated for the simulated middle-of-cycle condition depicted in Fig. 4. The calculated k-effective for the *critical* (k-effective experimental = 1.0) was 1.02389. The level of agreement between calculation and experiment was comparable to BOC conditions, yet with a differently signed bias. Note that the europium portion of the regulating/safety elements only extended 2 cm into the bottom and top of the fueled region of the core.

The *level of agreement* between calculated and measured local power density distribution is shown in Fig. 10. As for BOC, the greatest discrepancies are at the edges—both radial and axial—of the fuel elements. However, the magnitudes of the differences are reduced. Note that the largest magnitude of under-prediction of local power density is near to the europium portion of the regulating and safety elements.

Tables 3 and 4 show the measured and calculated streak factors. Data from these tables are plotted in Fig. 11. The level of agreement for streak factors is excellent. Variations of up to 7% can be expected not only because of the previously stated (Sect. 3.1.1) uncertainty in the measured local power density values but also because another 2–3% normalization error (maximum and negative; calculated values usually

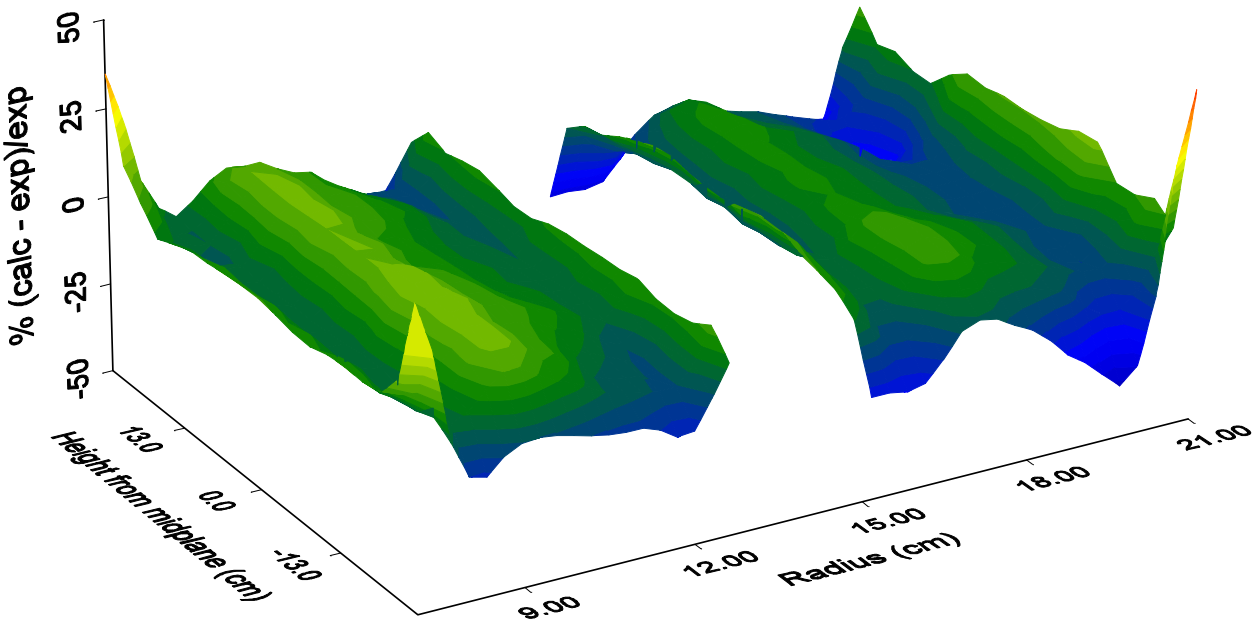

Fig. 10. Level of agreement between calculation and experiment for middle-of-cycle configuration.

Table 3. Measured streak factors from Fig. 4 (simulated middle of cycle)

Radius (cm)	Relative streak factor
7.14	1.2751
8.0	1.0931
9.0	0.9825
10.0	0.9712
11.0	0.9835
12.0	1.0201
12.6	1.0734
15.15	1.1029
16.0	1.0703
17.0	1.0163
18.0	0.9571
19.0	0.9335
20.0	0.9548
21.0	0.9561

Table 4. Calculated streak factors for Fig. 4

Radius	Relative streak factor
7.320	1.257
7.750	1.169
8.250	1.097
9.000	1.030
10.000	1.003
11.000	0.996
11.750	1.003
12.300	1.040
15.325	1.098
15.750	1.073
16.250	1.059
17.000	1.024
18.000	0.963
19.000	0.928
19.750	0.920
20.250	0.922
20.750	0.936

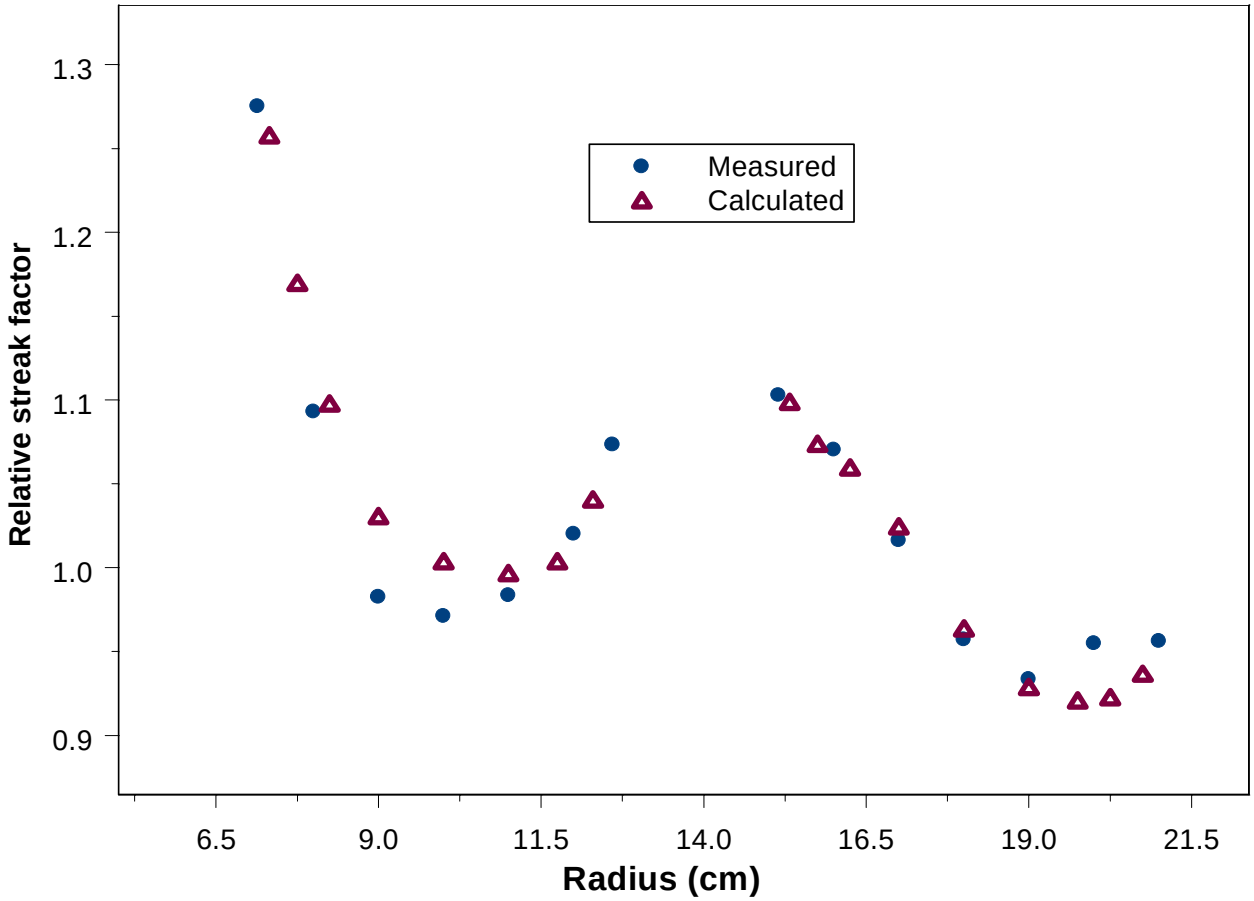

Fig. 11. Comparison of measured and calculated streak factors for middle of cycle.

low) is introduced into the calculated local power densities by selecting the mesh point closest to the measured mesh point rather than integrating over a volume corresponding to the volume associated with the "measured" mesh point.

The magnitude of the measured hot spot (from Fig. 4) is 1.67 at the midplane at the inside edge of the inner element (radius = 7.14 cm, axial heights of 0). The calculated hot spot location is at the same location. The magnitude of the calculated hot spot was 1.74. This discrepancy of 4% was in agreement with that expected from experimental uncertainty and is conservative. These comparisons indicate that the ability to calculate the hot spot location and magnitude and hot streak factor are comparable to or better than that for beginning of life.

3.2.2 Reduced-Tantalum-Content Regulating/Safety Elements

3.2.2.1 Calculated physics parameters for configuration critical with existing regulating/safety element design

Following the procedure described in Sect. 3.1, the reactor model used for the calculations reported in Sect. 3.2.1 (Fig. 4 configuration) was modified to reduce the tantalum content of both the regulating and safety elements from 38 vol % to 30 vol %. The locations of the control and safety elements were unchanged.

The calculated k-effective was 1.02884. Assuming an effective delayed neutron fraction for the HFIR fuel of 0.0076, the change in reactivity from the 38 vol % tantalum case due to reducing the tantalum content was 65 cents.

The differential worth of the existing regulating/safety element combination with elements withdrawn to 54.1 cm (21.295 in.) is 202 cents/in. (from Fig. 9). The change in tantalum content corresponds to a joint regulating/safety withdrawal of 0.32 in.—almost the same value as found for the BOC calculation.

The calculated hot streak factor for this configuration was slightly less than the calculated value for the 38 vol % control rod case (1.246) but at the same location. The location of the calculated hot spot factor was unchanged, but the magnitude was very slightly reduced (1.709).

3.2.2.2 Expected middle-of-cycle configuration for reduced-tantalum-content regulating/safety elements

The middle-of-cycle regulating/safety element withdrawal level was predicted by determining a calculated k-effective equal to the value noted in Sect. 3.2.1 (the critical Fig. 4 configuration). An element withdrawal of 20.99 in., that is, inserted 0.3-in. from the existing control element critical configuration, was found to yield a k-effective of 1.02391, only 0.002% different from the "critical" value found for the existing regulating/safety element design.

Local power densities for this new critical configuration were calculated and compared to the calculated values for the existing regulating/safety element design (Sect. 3.2.1 calculations). The location of the hot streak factor was unchanged and the magnitude was insignificantly different. The location and magnitude of the calculated hot spot were unchanged from the values for the Fig. 4 configuration. The value of the calculated, relative local power density at the measured hot spot location was 1.74—the same as the value calculated for the critical configuration of Fig. 4. Comparing the critical configuration with 38 vol % tantalum to the critical configuration with 30 vol % tantalum, the value of the calculated relative local power density at the inside edge of the inner fuel element at the base of the element—the outlet location for both the measured and calculated hot streaks—was insignificantly larger (increased by 1%).

3.2.3 Differential Element Worth for Middle-of-Cycle Conditions

From Fig. 9, the differential element worth for the current regulating/safety elements at an element withdrawal of 21.295 in. (the value for Fig. 4), was 202 cents/in. The positions of the regulating and safety elements in the computational model for Fig. 4 (Sect. 3.2.1) were computed and compared to the measured data from Fig. 9. The calculated differential worth was 232 cents/in. (113 cents/in. for the four safety plates and 119 cents/in. for the regulating element). Thus, the bias in the differential worth calculation for middle-of-cycle is 30 cents/in. The differential worth at middle-of-cycle configuration for the reduced-tantalum-content elements is 227 cents/in. (107 cents/in. for the four safety plates and 120 cents/in. for the regulating element).

3.2.4 Conclusions Regarding the Use of Reduced-Tantalum-Content Regulating/Safety Elements at Middle-of-Cycle

The expected change in midcycle regulating/safety element withdrawal position for the reduced-tantalum-content elements vs the current design is –0.3 in. The magnitudes and locations of the hot streak and hot spot factors for a middle-of-cycle critical configuration with the reduced-tantalum regulating/safety elements are unchanged from the values for the middle-of-cycle critical configuration with the existing regulating/safety elements. The differential regulating/safety element worth at the middle-of-cycle critical configuration for the reduced-tantalum elements is essentially the same as the differential worth for the existing regulating/safety elements at the middle-of-cycle critical configuration for those elements.

3.3 SIMULATED NEAR-END-OF-CYCLE (EOC) CONDITION

3.3.1 Validation with Existing Regulating/Safety Element Configuration

The analyses discussed in Sect. 3.1 were repeated for the simulated near-EOC condition depicted in Fig. 5. The calculated k-effective for the *critical* (k-effective experimental = 1.0) was 1.03058. The level of agreement between calculation and experiment was somewhat improved from BOC conditions, but the discrepancy between measured and calculated was higher than would be expected based on calculation of other, HEU critical experiments.

The *level of agreement* between calculated and measured local power density distribution is shown in Fig. 12. As found for previous calculations, the greatest discrepancies are at the edges—both radial and axial—of the fuel elements. The magnitudes of the differences are similar to those seen in Fig. 10 for middle-of-cycle.

Tables 5 and 6 show the measured and calculated streak factors. Data from these tables are plotted in Fig. 13. The level of agreement for streak factors is excellent.

The magnitude of the measured hot spot (from Fig. 5) is 1.57 at the midplane at the inside edge of the inner element (radius = 7.14 cm, axial height of 0). The calculated value of the relative local power density at that location is 1.598, which agrees with the measured value within measurement uncertainty.

The magnitude of the calculated hot spot was 1.67 at a radius of 20.95 cm and axial location of 0.0 cm (midplane of the outside edge of the outer element). The corresponding measured value at that location was 1.55. This discrepancy of 7.7% was slightly greater than expected from experimental uncertainty but is conservative. These comparisons indicate that the ability to calculate the hot spot location and magnitude was comparable to that of the hot streak factor.

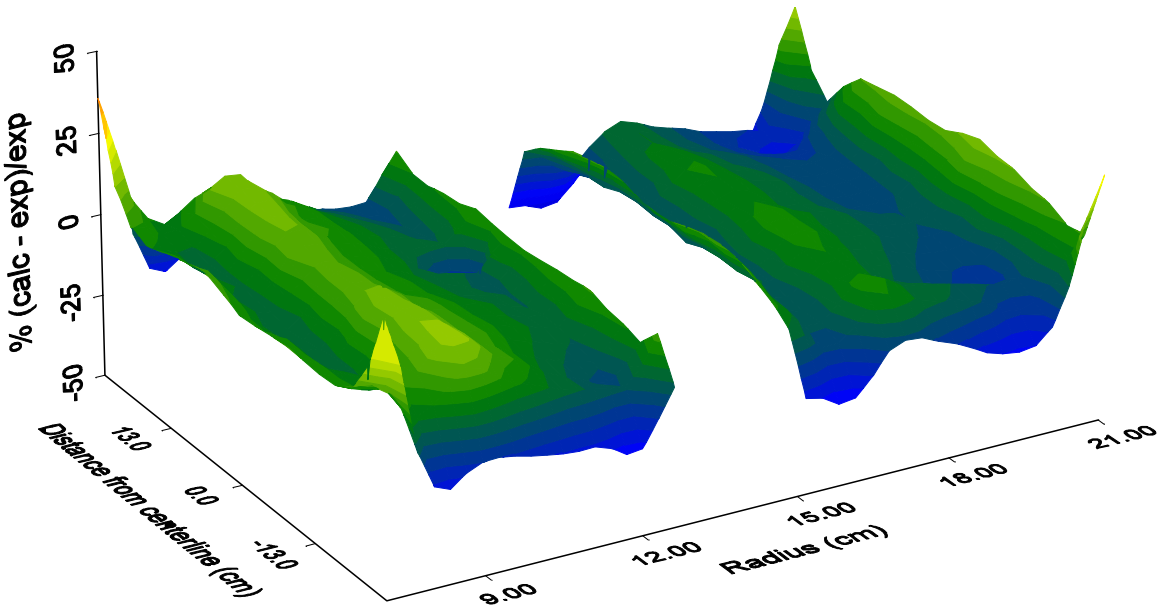

Fig. 12. Level of agreement between calculation and experiment for near-EOC configuration.

Table 5. Measured streak factors from Fig. 5 (simulated near-EOC)

Radius (cm)	Relative streak factor
7.14	1.1814
8.0	0.9970
9.0	0.9136
10.0	0.9169
11.0	0.9293
12.0	0.9679
12.6	0.9999
15.15	1.0425
16.0	1.0360
17.0	1.0108
18.0	0.9779
19.0	0.9809
20.0	1.0332
21.0	1.1196

Table 6. Calculated streak factors for Fig. 5

Radius	Relative streak factor
7.320	1.175
7.750	1.087
8.250	1.018
9.000	0.957
10.000	0.935
11.000	0.932
11.750	0.939
12.300	0.973
15.325	1.041
15.750	1.027
16.250	1.024
17.000	1.009
18.000	0.975
19.000	0.979
19.750	1.010
20.250	1.044
20.750	1.097

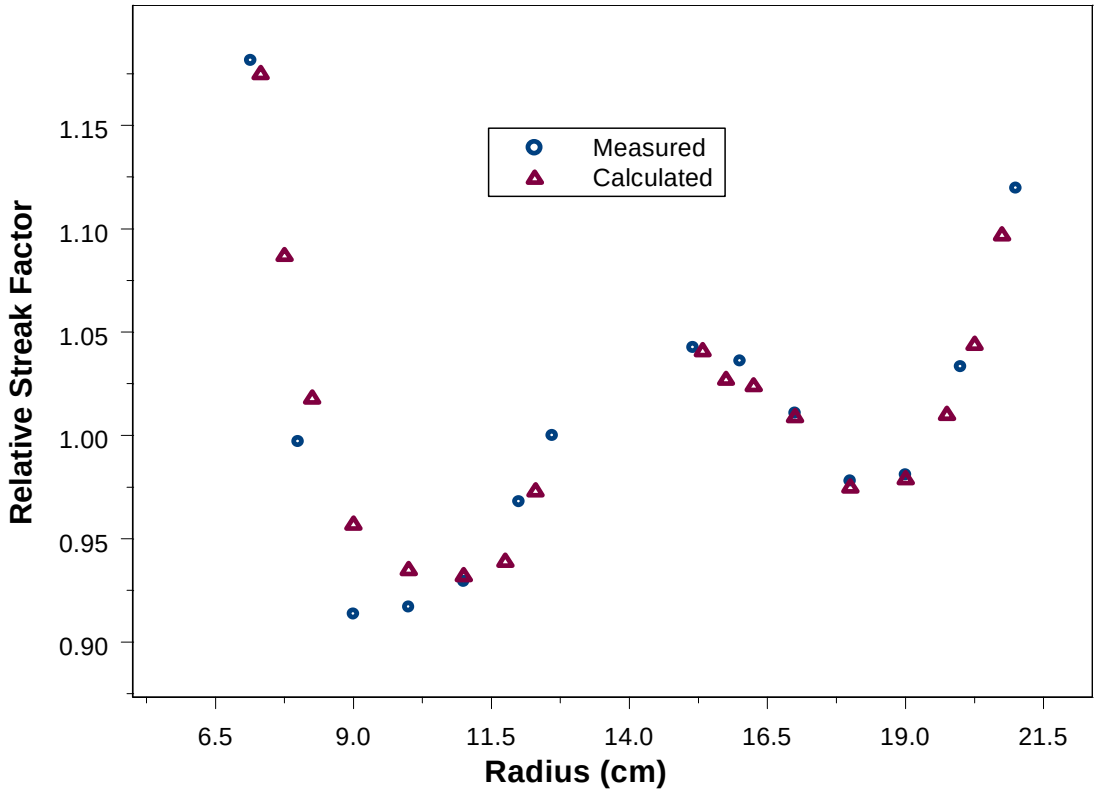

Fig. 13. Comparison of measured and calculated streak factors for near-EOC.

3.3.2 Reduced-Tantalum-Content Regulating/Safety Elements at Near-EOL

3.3.2.1 Calculated physics parameters for configuration critical with existing regulating/safety element design

Following the procedure described in Sect. 3.1, the reactor model used for the calculations reported in Sect. 3.3.1 (Fig. 5 configuration) was modified to reduce the tantalum content of both the regulating and safety elements from 38 vol % to 30 vol %. The location of the control elements was unchanged.

The calculated k-effective was 1.03238. Assuming an effective delayed neutron fraction for the HFIR fuel of 0.0076, the change in reactivity from the 38 vol % tantalum case due to reducing the tantalum content was 22 cents.

The differential worth of the existing regulating/safety element combination with elements withdrawn to 61.7 cm (24.3 in.) is 118 cents/in. The change in tantalum content corresponds to a joint regulating/safety withdrawal of –0.19 in.—slightly less than that found for the BOC and middle-of-cycle calculations.

The calculated hot streak factor for this configuration was slightly less than the value for the 38 vol % control rod case (1.169) but at the same location. The location of the calculated hot spot factor was unchanged, but the magnitude was very slightly reduced (1.658).

3.3.2.2 Expected near-EOC configuration for reduced-tantalum-content regulating/safety elements

The near-EOC regulating/safety element withdrawal level was predicted by determining a calculated k-effective equal to the value noted in Sect. 3.3.1 (the critical Fig. 5 configuration). An element

withdrawal of 24.0 in., that is, inserted 0.3 in. from the existing control element critical configuration, was found to yield a k-effective of 1.03009, only 0.05% different from the "critical" value found for the existing regulating/safety element design.

Local power densities for this new critical configuration were calculated and compared to the measured local power densities for the existing regulating/safety element design (Sect. 3.3.1 calculations). The location and magnitude of the hot streak factor were unchanged (same as in Table 6). The location and magnitude of the calculated hot spot were unchanged from the values for the Fig. 5 configuration. The value of the calculated, relative local power density at the measured hot spot location was 1.598—the same as the value calculated for the critical configuration of Fig. 5.

Comparing the critical configuration with 38 vol % tantalum to the critical configuration with 30 vol % tantalum, the value of the calculated relative local power density at the inside edge of the inner fuel element at the base of the element—outlet location for both the measured and calculated hot streaks—increased slightly. The value changed from 0.837 to 0.847, an increase of 1.2%.

3.3.3 Differential Element Worth for Near-EOC Conditions

From Fig. 9, the differential element worth for the current regulating/safety elements at an element withdrawal of 24.3 in. (the value for Fig. 5), was 118 cents/in. The positions of the regulating and safety elements in the computational model for Fig. 5 were modified so that a differential worth value could be computed and compared to the measured data from Fig. 9. The calculated differential worth for the current elements was 103 cents/in. (50 cents/in. for the four safety plates and 53 cents/in. for the regulating element). The bias in the differential worth calculation for near-EOC was –15 cents, less than that found for middle-of-life calculations.

The differential worth at near-EOC configuration for the reduced-tantalum-content elements was 100 cents/in. (51 cents/in. for the four safety plates and 49 cents/in. for the regulating element).

3.3.4 Conclusions Regarding the Use of Reduced-Tantalum-Content Regulating/Safety Elements at Near-EOC

The expected change in near-EOC regulating/safety element withdrawal position for the reduced-tantalum-content elements vs the current design is –0.2 in. The magnitudes and locations of the hot streak and hot spot factors for a near-EOC critical configuration with the reduced-tantalum regulating/safety elements are unchanged from the values for the near-EOC critical configuration with the existing regulating/safety elements. The differential regulating/safety element worth at the near-EOC critical configuration for the reduced-tantalum elements is essentially the same as the differential worth for the existing regulating/safety elements at the near-EOC critical configuration for those elements.

4. SAFETY ANALYSES FOR REDUCED-TANTALUM CONTROL/SAFETY ELEMENTS

The neutronics studies in Sect. 3 showed that the power distributions in the reactor core, as a function of burnup, are not significantly perturbed due to the planned reduction in tantalum content from 38 vol % to 30 vol %. The word "significantly" should be interpreted to mean that the computed difference in critical power distributions between the reduced tantalum content and existing control/safety elements is less than one standard deviation from measurements of local power densities that were made in various critical experiments.

For beginning-, middle- and near-EOL control/safety element critical configurations, the differential worth of the reduced-tantalum control and safety elements (combined) was shown to be the same (around the critical configuration) as for the current (38 vol % tantalum) control and safety elements at their critical configurations. However, for all three points in the life cycle of the fuel elements, the difference in element insertion position for a critical configuration for the reduced-tantalum-content elements was always 1/3-in. or less than that for the critical configuration with the existing elements. That is, the elements were withdrawn less for the reduced-tantalum elements than for the existing elements, and the amount was always 1/3 in. or less.

Steady-state and transient analyses that are documented or referenced in the *HFIR Updated Safety Analysis Report* (USAR) are based on computer models described in refs. 10–12. The power distributions that are input to the program described in ref. 10 are calculated distributions that are documented in ref. 2. Calculations reported in Sect. 3 indicate that these distributions should be essentially unchanged for critical configurations corresponding to the reduced-tantalum-content elements. The power distributions that are input to the RELAP[13] models for various safety analyses show that HFIR operations are safe under all normal and design basis accident conditions.* The studies reported in Sect. 3 show that the variations in hot channel and hot spot factors due to tantalum reduction are much less than the experimental uncertainties associated with these numbers (both at the measured locations from the critical experiments and at the calculated locations). Consequently, one can conclude that there is not a reduction in the margin of safety for nominal or design basis accident conditions due to changes in the power distribution caused by a reduction in tantalum.

4.1 REACTIVITY WORTH ESTIMATES—SAFETY ANALYSIS REPORT CHAPTER 15 REQUIREMENTS

The Updated Safety Analysis Report (ref. 14) is a basis for defining transients and accidents to which the control system must be capable of responding. Section 15.2.1 of that reference notes that the *Nuclear Regulatory Commission Guide 1.70* recommends the analysis of events in eight categories. These include

1. increase in secondary heat removal,
2. decrease in secondary heat removal,
3. decrease in reactor coolant system flow rate,
4. reactivity and power distribution anomalies,
5. increase in reactor primary coolant inventory,
6. decrease in reactor primary coolant inventory,
7. radioactive releases from a subsystem or component, and
8. anticipated transients without scram.

*Internal communication from J. D. Freels and K. A. Smith, Research Reactors Division, ORNL (internal document, C-HFIR-1998-001, and references noted in that document).

Item 7 is not related to reactivity control and thus is independent of the proposed change in tantalum content. Items 1–3, 5–6, and 8 concern conditions in which the transient is assumed to not perturb the power distribution in the reactor core. That is, reactor kinetics calculations are not performed in the transient analyses documented in the HFIR Safety Analysis Report. For Cases 1–3 and 5–6, the power distribution is assumed to be in a steady state critical configuration and, when the transient condition occurs and the safety plates scram, the decay heat generation is in the same distribution as the steady state power distribution. For Case 8, of course, there is not a scram.

As noted in Sect. 3 of this report, for equivalent—meaning equivalent burnup in the fuel cycle—critical configurations for 38 and 30 vol % tantalum elements, the differential worth of the 38 and 30 vol% elements will be the same. Consequently the response of the reactor power to the insertion of the safety plates for these transients will be unchanged for 30 vol % elements relative to the response for 38 vol % elements. Note also that the shutdown worth of the 30 vol % elements will be the same as for the 38 vol % elements because the shutdown worth is dependent solely on the europium content and configuration in the elements and these are unchanged between designs. It is also noteworthy that, for equivalent burnups in the fuel cycle, there are no significant changes in the reactor power distributions between the 30 and 38 vol % designs. Consequently, the proposed change in the tantalum content of the control element will not impact the safety-related analyses for any of items 1–3, 5–6, and 8.

Regarding item 4, reactivity and power distribution anomalies, ref. 14 identifies five cases for evaluation:

- Case 0, approach to nominal steady state,
- Case 1, pump start in cold idle heat exchanger loop,
- Case 2, excess withdrawal of four safety plates and control cylinder,
- Case 3, ejection of control cylinder, and
- Case 4, generation of void in the target region.

4.1.1 Expected, Nominal Control and Safety Element Operation

Integral worth data for symmetric control and safety element movement is shown in Tables 7 (for 38 vol % tantalum elements) and 8 (for 30 vol % elements). Table 7 presents the integral worth of existing 38 wt % tantalum elements obtained by integrating Fig. 9. Table 8 presents the integral

Table 7. Integral control element worths for 38 vol % tantalum elements (integral of Fig. 9)

Inches inserted	Inches withdrawn	Control element worth ($)	Four safety element worth ($)
0.0	27.00	0.0	0.0
0.500	26.50	–0.285	–0.285
1.500	25.50	–0.695	–0.695
2.500	24.50	–1.240	–1.240
3.500	23.50	–1.935	–1.935
4.500	22.50	–2.780	–2.780
5.500	21.50	–3.765	–3.765
6.500	20.50	–4.875	–4.875
7.500	19.50	–6.120	–6.105
8.500	18.50	–7.500	–7.440
9.500	17.50	–9.005	–8.860
10.500	16.50	–10.625	–10.350
11.500	15.50	–12.345	–11.890
12.500	14.50	–14.155	–13.460
13.500	13.50	–16.040	–15.050
14.500	12.50	–17.980	–16.650
15.000	12.00	–18.960	–17.450

Table 8. Integral control element worths for 30 vol % tantalum elements

Inches inserted	Inches withdrawn	Control element worth ($)	Four safety element worth ($)
0.0	27.0	0.0	0.0
0.833	26.17	–0.285	–0.285
1.833	25.17	–0.695	–0.695
2.833	24.17	–1.240	–1.240
3.833	23.17	–1.935	–1.935
4.833	22.17	–2.780	–2.780
5.833	21.17	–3.765	–3.765
6.833	20.17	–4.875	–4.875
7.833	19.17	–6.120	–6.105
8.833	18.17	–7.500	–7.440
9.833	17.17	–9.005	–8.860
10.833	16.17	–10.625	–10.350
11.833	15.17	–12.345	–11.890
12.833	14.17	–14.155	–13.460
13.833	13.17	–16.040	–15.050
14.833	12.17	–17.980	–16.650
15.000	12.00	–18.960	–17.450

worth of the reduced-tantalum elements. For the reduced-tantalum control elements, the curves are generated by assuming that the differential curves in Fig. 9 are shifted left by 1/3 in. and the worth at 15 in. inserted is assumed to be the same as for the 38% tantalum elements because at that point the europium regions of the elements begin to overlap. Note that the values at the "end points" (fully withdrawn and 15 in. inserted) are estimates based on tying the calculations reported in Sect. 3 to known reactivity values. If needed, more accurate estimates could be generated from the calculational models described in this document. Data from Tables 7 and 8 are plotted in Figs. 14 and 15. The change in the integral rod worth curve due to the reduction of tantalum means that the procedure for estimating the symmetric critical control element position will have to be revised prior to loading the reduced-tantalum-content control elements to the reactor.*,†

4.1.1.1 Changes in reactivity worth due to burnup

For the existing control element design (38 vol % tantalum), it is obvious that at some point during the irradiation cycle for the control elements, the tantalum concentration will be 30 vol % tantalum. This experience base cannot, by itself, certify the acceptability of reducing the tantalum content in the control elements because during irradiation, the europium region of the control element is also undergoing changes. Significant quantities of gadolinium isotopes, some having absorption cross section values significantly higher than the europium isotopes in the fresh elements, are generated (see ref. 15). The changes in the europium lead to reactivity changes that mask the reactivity changes due to the depletion of tantalum.

*K. A. Smith, "Procedure for Determining the Beginning-of-Cycle ESCCEP of HFIR Control Plates," RTP-2, RRD Document Control Center, August 22, 2001.

†The acceptance criteria for predicting symmetric, critical control element position is 0.5 in. Every time the safety plates are replaced, a change of approximately 0.4 in. is seen, and this is not taken into account in the thermal-hydraulic model (nor does it need to be).

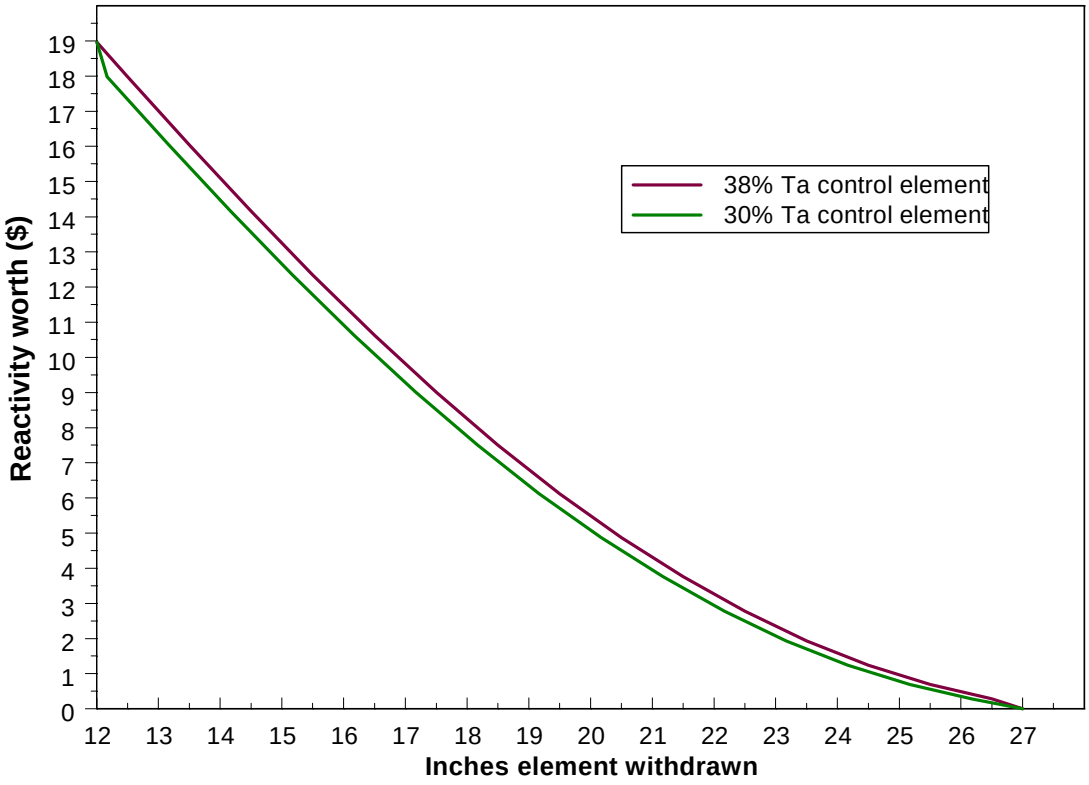

Fig. 14. Integral control element worths.

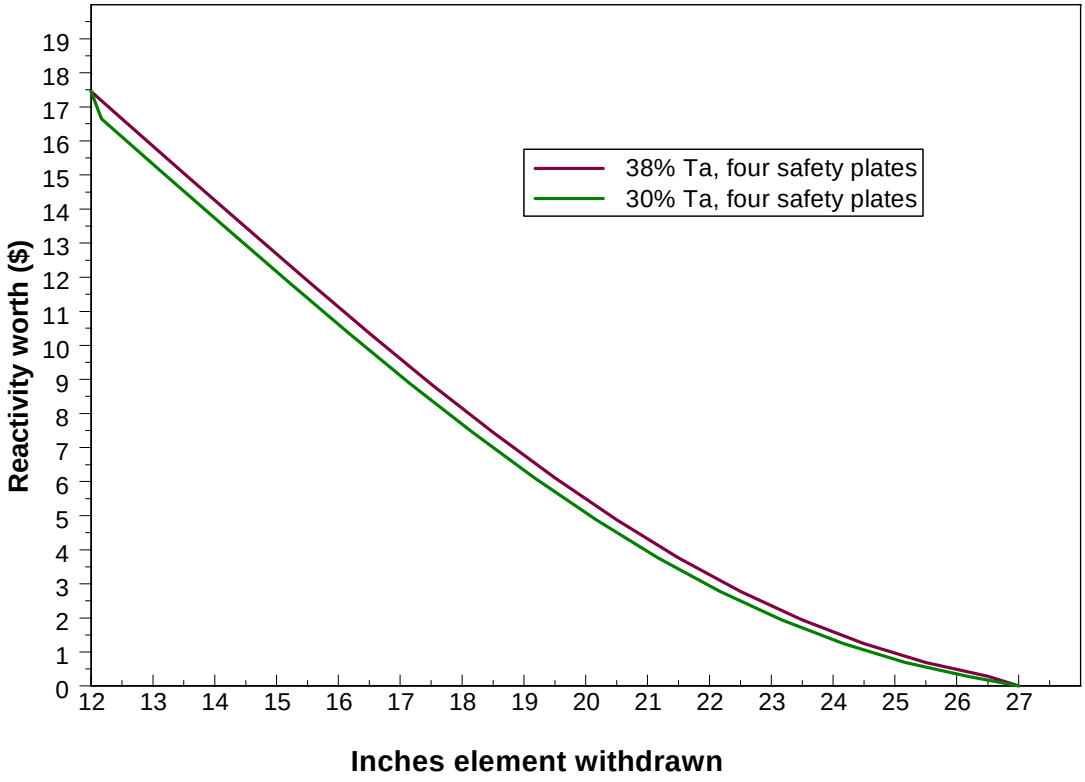

Fig. 15. Integral four safety plate worths.

Reference 15 notes “Some cylinders … have been exposed to well over one year of full-power service (>35,000 MWd) with no indications of operational problems or significant change in nuclear worth.” Recent experience at HFIR also shows that the worth of the control and safety elements is essentially unchanged during their irradiation cycle. The startup symmetric critical control element position for cycle 389 when the four safety plates had exposures ranging from 38,106 to 40,496 MWd was 18.36 in. The startup symmetric critical control element position for cycle 390, which had four, fresh safety plates and essentially the same experiment loading was 18.13 in. This difference corresponds to approximately 70 cents of reactivity and is well within the margin of uncertainty allowed for the prediction of startup symmetric control positions (0.5 in. according to RRD procedures). For cycles 388–395, the average variation between predicted and actual startup symmetric element position was ±0.11 in.

To estimate the EOL relative worth of control/safety elements, depletion calculations for the tantalum (30 vol %) region of the elements are performed by coupling the nuclear-data-library-generation data sets, described in Sect. 2, for BOL conditions, described in Sect. 3, to the ORIGEN-S program (a part of the SCALE computational system). Calculations for that portion of the europium region that is adjacent to the tantalum region (0.5 in. from the Ta/Eu interface) are also performed. These data sets are included in Appendix A. Validation studies for the ORIGEN calculations are discussed in Appendix E. Fresh and EOL (100,000-MWd) atom densities are reported in Table 9. Only 45% of the tantalum is transmuted during irradiation of the control/safety elements.

Table 9. Changes in control element isotopics due to irradiation

Nuclide	Atom density in fresh control elements [atoms/(bn*cm)]	Atom density in control elements at 100,000 MWD [atoms/(bn*cm)]
Tantalum region		
^{181}Ta	$1.5020(10^{-2})$	$8.24(10^{-3})$
^{182}Ta	–	$1.74(10^{-5})$
^{183}Ta	–	$3.02(10^{-5})$
^{180}W	–	$2.23(10^{-7})$
^{181}W	–	$2.97(10^{-8})$
^{182}W	–	$7.75(10^{-5})$
^{183}W	–	$4.19(10^{-3})$
^{184}W	–	$2.52(10^{-3})$
^{185}W	–	$1.45(10^{-5})$
^{186}W	–	$1.46(10^{-6})$
Europium region at 1.3 cm from Eu/Ta interface		
^{151}Eu	$3.83195(10^{-3})$	$1.43(10^{-3})$
^{152}Eu	–	$6.64(10^{-4})$
^{153}Eu	$4.12667(10^{-3})$	$3.00(10^{-3})$
^{154}Eu	–	$1.02(10^{-3})$
^{155}Eu	–	$7.04(10^{-5})$
^{156}Eu	–	$1.32(10^{-5})$
^{152}Gd	–	$5.56(10^{-4})$
^{153}Gd	–	$1.73(10^{-5})$
^{154}Gd	–	$1.57(10^{-4})$
^{155}Gd	–	$9.61(10^{-6})$
^{156}Gd	–	$3.88(10^{-4})$
^{157}Gd	–	$9.30(10^{-7})$
^{158}Gd	–	$4.12(10^{-6})$

Absorption cross sections for selected nuclides present in the irradiated tantalum portion of the control/safety elements are shown in Fig. 16. The large value for ^{182}Ta results in this nuclide contributing significant neutron poisoning in spite of its relatively small concentration. Various tungsten isotopes also have significant absorption cross sections though generally not as large as ^{181}Ta. It will be shown in Sect. 4.1.4.2 that the presence of ^{182}Ta and tungsten isotopes in the irradiated tantalum-bearing region lead to a calculated EOL reactivity worth that is larger than that of the fresh tantalum region. Because HFIR safety analysis report (SAR) analyses are based on unirradiated tantalum isotopics, the actual EOL control and safety element worth due to the tantalum region will be greater than has been assumed in the analyses documented in the SAR.

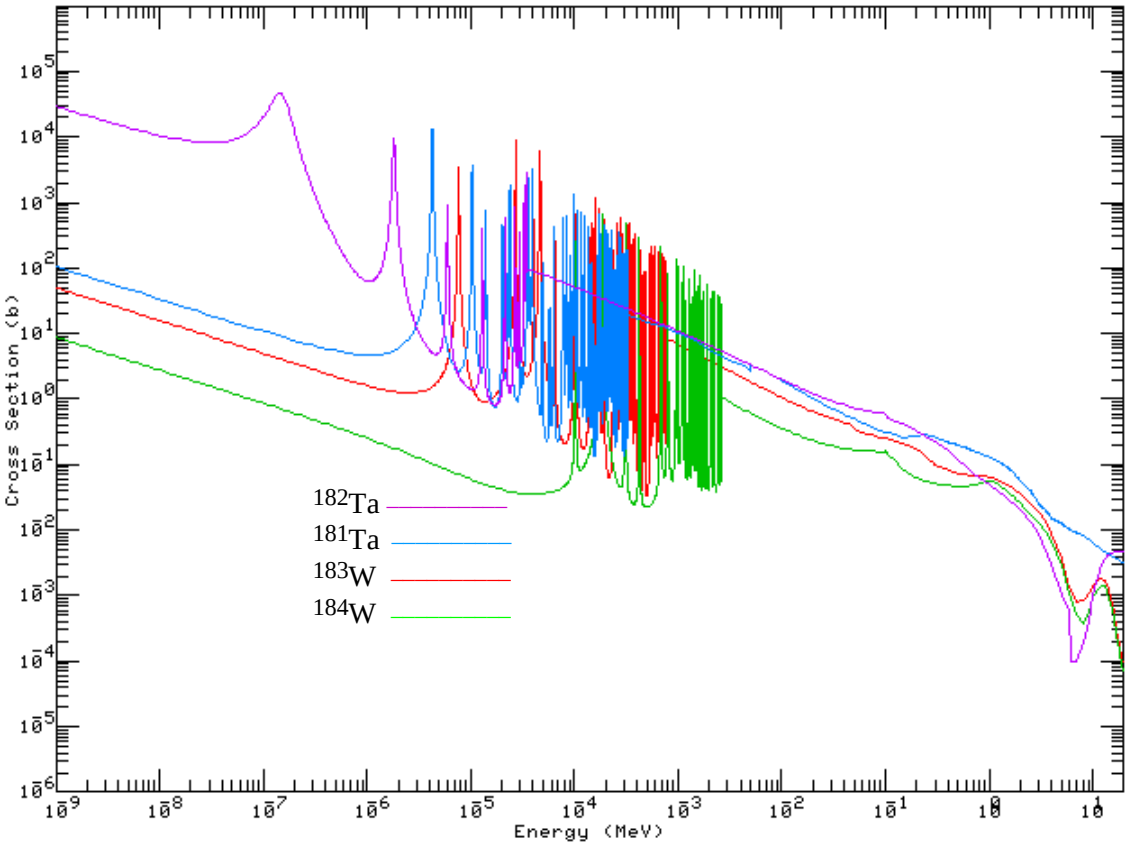

Fig. 16. Microscopic absorption cross sections for selected nuclides.

4.1.1.2 Shutdown reactivity worth

The shutdown worth of the HFIR control and safety elements is due to the europium portion of the elements being adjacent to the fueled region of the element over the entire axial extent of the fuel. Consequently, the shutdown worth of the elements is unchanged by the reduction in the tantalum content.

4.1.2 Pump Start in Cold Loop

This transient concerns the insertion of cold water into the reactor core with consequent positive reactivity insertion due to the negative temperature coefficient of the fuel. For the cold loop pump start

and optimum void events, the reactor is simply assumed to be critical without regard for the position of the control elements.

For the reduced-tantalum elements, the following assumptions regarding the transient are unchanged from the existing control element configuration: value of fuel and moderator temperature coefficients, amount of reactivity insertion, response (speed) of control and safety systems, and differential worth of control and safety plates from their pretransient, critical locations. Given that these conditions are unchanged, the results of the safety-related analyses, documented in ref. 14, are also unchanged.

4.1.3 Void Generation in the Target Region

This transient concerns the insertion (transport via coolant) of a bubble (or void) into the central target region of the reactor with consequent positive reactivity insertion due to removal of hydrogen moderation (the neutrons are no longer "trapped" in the "flux trap"). For the reduced-tantalum elements, the following assumptions regarding the transient are unchanged from the existing control element configuration: value of the target void coefficient, value of fuel and moderator temperature coefficients, amount of reactivity insertion, response (speed) of control and safety systems, and differential worth of control and safety plates from their pretransient locations. Given that these conditions are unchanged, the results of the safety-related analyses, documented in ref. 14, will also be unchanged.

4.1.4 Control Element Ejection

According to the HFIR Safety Analysis Report, Sect. 15.3.4.3 (ref. 14), the limiting transient event in terms of reactivity insertion for the existing regulating and safety elements is a control (regulating) element ejection accident. In this scenario, the four safety plates are assumed to initially be at 26.86 in. withdrawn (fully withdrawn) position and are then inserted at their nominal travel from that position on reactor scram. The control cylinder is assumed to initially be at 16.0 in. withdrawn (point of maximum differential worth) and to travel at 0.662 in./s downward (withdrawn) until it is fully withdrawn (at 26.86 in.).

4.1.4.1 Fresh (design basis) control and safety elements

The computational model for this transient requires as input, the integral "rod" worth data for the control and safety elements as a function of position. For the existing, 38 vol % control elements, these data are provided in Table 10 and shown in Fig. 17.

For a reduced-tantalum control element, the point of maximum differential worth will be shifted slightly (one-third inch less withdrawn based on the results of the studies reported in Sect. 3). The differential worth of withdrawing the regulating element will be the same as for the existing regulating elements (due to the differential worth at corresponding critical configurations being the same). Consequently, the data for a regulating element with reduced tantalum can be assumed to be the same as in Table 10 but with positions adjusted by 1/3 in. The progression of the reactivity portion of the transient due to the control element will be unchanged from the analyses documented in the USAR.

For the reduced-tantalum safety elements, the differential worth of those elements will be different from that of 38 vol % elements. A series of calculations based on the BOL DORT model described in Sect. 3.1.2 was conducted so that the reactivity impacts of the reduced tantalum content of both the control and safety elements could be properly accounted. The control element was assumed to be inserted to 15.7 in. (1/3 in. further than for the existing element), and the transient was assumed to progress according to the scenario described previously.

Calculated differential worth is shown in Table 11. This differential worth is compared to the measured, symmetric four safety plate worth (from Fig. 9) in Fig. 18. Integral worth data from Table 11—computed by step-wise integration of the differential data—are plotted in Fig. 19 along with the USAR safety element assumption (shown in Fig. 17). Note that the data presented in Table 11 are derived from

Table 10. Integral worth of control elements for analyses in HFIR USAR (ref. 14)[a]

Inches inserted	Regulating element	Four safety plates
0.0000	0.0000	0.00000
0.5430	–0.1071	–0.07833
1.0860	–0.2476	–0.18291
1.6290	–0.4284	–0.31909
2.1720	–0.6551	–0.49111
2.7150	–0.9317	–0.70237
3.2580	–1.2611	–0.95569
3.8010	–1.6456	–1.25346
4.3440	–2.0871	–1.59773
4.8870	–2.5867	–1.99024
5.4300	–3.1457	–2.43236
5.9730	–3.7647	–2.92495
6.5160	–4.4442	–3.46822
7.0590	–5.1844	–4.06143
7.6020	–5.9847	–4.70255
8.1450	–6.8439	–5.38790
8.6880	–7.7598	–6.11166
9.2310	–8.7286	–6.86532
9.7740	–9.7448	–7.63706
10.317	–10.8008	–8.41110
10.860	–11.8859	–9.16695
18.86	–	–13.84
19.86	–16.63	–
26.86	–16.63	–13.84

[a]Effective delayed neutron fraction assumed to be 0.0076.

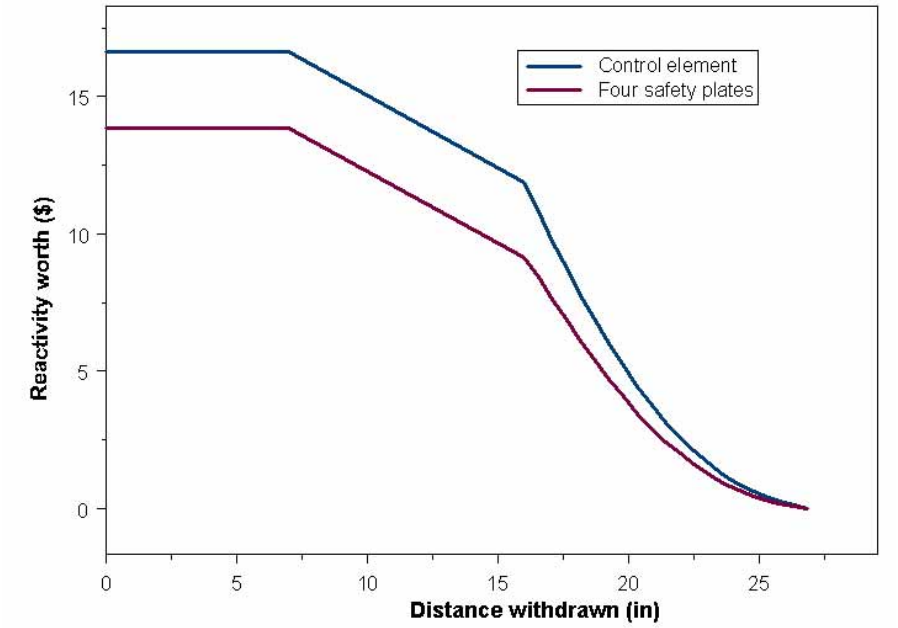

Fig. 17. Assumed integral reactivity worth of 38 vol % tantalum elements for HFIR USAR analyses (ref. 14).

Table 11. Differential and integral four-safety-plate worths for 30 vol % tantalum elements for control element ejection case

Inches inserted	Inches withdrawn	Differential worth (cents/in.)	Integral worth ($)
0.25	26.75	15.55	0.16
1.0	26.00	39.52	0.25
2.0	25.00	56.85	0.73
3.0	24.00	72.27	1.37
4.0	23.00	92.43	2.20
5.0	22.00	111.23	3.21
6.0	21.00	133.39	4.44
7.0	20.00	143.73	5.82
8.0	19.00	151.92	7.30
9.0	18.00	151.03	8.82
10.0	17.00	150.48	10.32
11.0	16.00	152.24	11.84
12.0	15.00	147.27	13.34
13.0	14.00	134.43	14.74
14.0	13.00	101.26	15.92
15.0	12.00	86.20	16.86
16.0	11.00	78.63	17.68
17.0	10.0	66.68	18.41
19.5	7.5	20.25	18.84
22.0	5.0	3.34	18.96
24.25	2.75	0.0	18.98

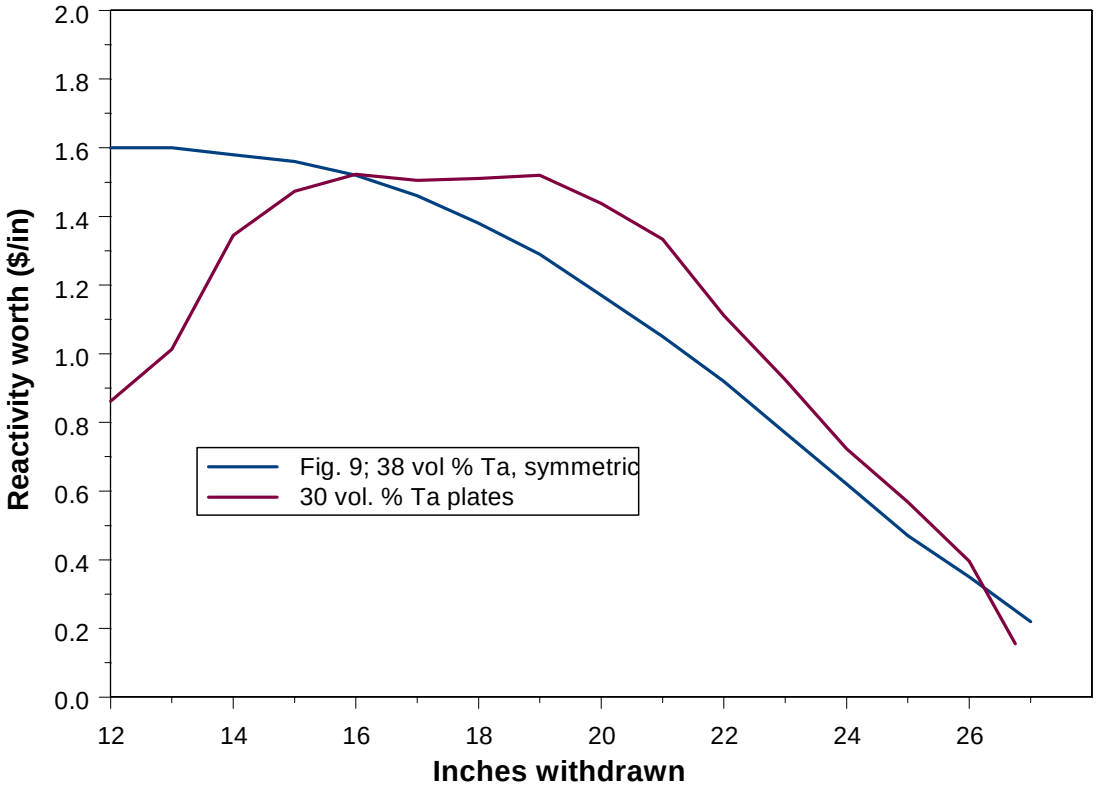

Fig. 18. Control element ejection case; comparison of four-safety-plate worths for existing, symmetric elements with 30 vol % tantalum safety plates.

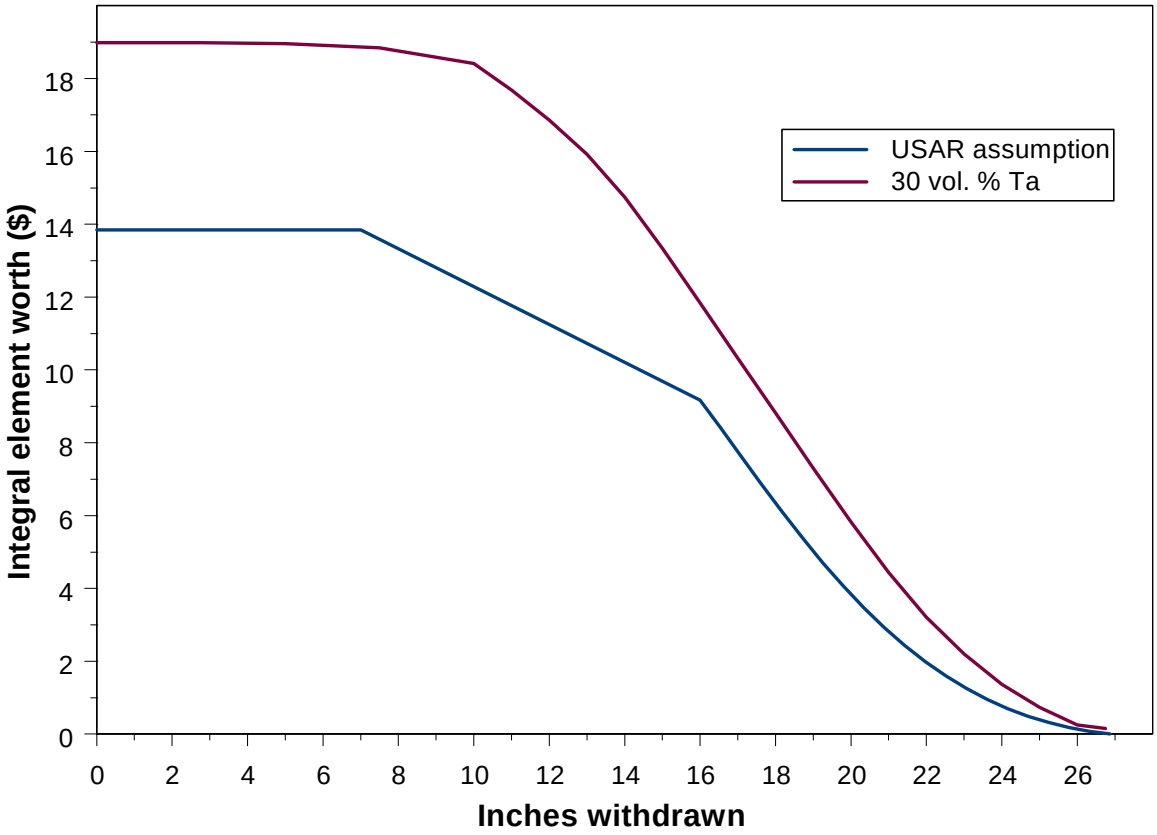

Fig. 19. Comparison of four-safety-plate worths for control element ejection with 30 vol % tantalum safety plates with USAR assumption.

calculations for the specific case of control element ejection (control element assumed not to move, safety plates inserted from "full out"). These data are not applicable to the excess withdrawal of safety or control plates (Sect. 4.1.3) because that transient starts from a symmetric critical configuration not asymmetric (the model for the calculations reported in Table 11).

For the differential worth data, the presence of the inserted control element skews the flux to the top of the core, therefore enhancing the safety element worth relative to the symmetric value measured in the critical experiment. The comparison of the integral worth curves shows the large degree of conservatism present in the HFIR USAR calculations even when considering the effect of the reduced-tantalum content.

The differential worth of the four safety plates begins to be reduced when the plates are withdrawn 15 in.—close to the value for the control element for this scenario (withdrawn 15.7 in.) At the safety plate withdrawal position of 15 in., the tantalum-aluminum interface is at 2 in. below the core midplane. The tantalum-aluminum interface for the control element at 15.7 in. withdrawn is at 1.3 in. above the core midplane (3.3 in. of overlap for the tantalum sections of the elements; more than in the Fig. 3, BOL configuration).

Because the four-safety-plate worths assumed in the analyses documented in the HFIR USAR are significantly less than the values for the reduced-tantalum elements, there will be no impact on the safety analyses due to reducing tantalum. The margin of safety will not be reduced.

4.1.4.2 Control and safety plates at end-of-plate life

Using the EOL atom densities in Table 9, the differential worth of EOL safety plates were recalculated. The calculated differential worth, along with the fresh element differential worth values from Table 11, are shown in Table 12. As would be expected from the discussion presented in Sect. 4.1.1.1, EOL incremental worth of the safety plates is greater than for fresh elements. If both the control and safety elements were at their respective EOLs, the differential worth of the control element would also be greater, but the "travel speed" of the safety plates is several orders of magnitude greater than the travel speed of the control element. The shutdown worths of the control and safety elements are essentially unchanged because the majority of the europium region of the elements is unchanged due to irradiation (ref. 15, neutron flux is low).

Table 12. Comparison of differential four-safety-plate worths for 30 vol % tantalum elements for fresh and EOL configurations

Inches inserted	Inches withdrawn	Fresh differential worth (cents/in.)	EOL differential worth (cents/in.)
0.25	26.75	15.55	42.9
1.0	26.00	39.52	53.7
2.0	25.00	56.85	70.9

4.1.5 Excess Withdrawal of Safety Plates and Control Cylinder

Section 15.3.4.0.4 of ref. 14 provides a description of this transient.

> During a reactor startup, the control system automatically withdraws the shim elements until a 10% power level (8.5 MW) is reached. Once at this power, the automatic startup halts and the power level is maintained by the regulating servo. To change the power, the desired power is input to the control system, which generates an error signal to drive the servo. When the regulating rod reaches the servo withdrawal limit, a shim withdrawal is requested. The operator then manually allows withdrawal of the shims until the control cylinder is back in range.
>
> A failure within the control system or an operator error can result in an uncontrolled withdrawal of the shims. This situation can occur at any power level or any time in core life. The reactor responds with an increase in power, the rate of which depends on the initial conditions, which, for this scenario, are assumed to exist at well-defined steady state. The control system attempts to reverse the shim elements at 110% of full power. If this reverse is not sufficient, the safety system responds with a number of possible reactor scram trips including flux-to-flow ratio, power rate, neutron power, reactor inlet temperature, or heat power.

For this accident, the analyses that support the documentation in the USAR are based on the assumptions that the positive reactivity input corresponds to the control and safety elements being initially at the points of maximum differential rod worth but that the negative reactivity insertion corresponds to the safety plates being scrammed from the fully withdrawn position. Such a configuration is physically impossible but is conservative in terms of predicting the degree to which reactor conditions approach safety margins.

For the reduced-tantalum elements, the following assumptions in the analyses supporting the USAR regarding the transient are unchanged from the existing control element configuration: amount of

reactivity insertion, response (speed) of control and safety systems, and differential worth of control and safety plates from their pretransient locations. The studies reported in Sect. 3 of this report showed that, for equivalent burnups, the differential worth of the control and safety elements are unchanged when the tantalum content is reduced. Consequently, the positive reactivity worth insertion will be unchanged from the values assumed in the USAR. The negative reactivity worth inserted by the reduced-tantalum elements will be the same as was presented in the previous section on the control element ejection accident. Consequently, the results of the safety-related analyses, documented in ref. 14, are also unchanged.

4.2 REACTIVITY WORTH ESTIMATES—SAFETY ANALYSIS REPORT CHAPTER 16 REQUIREMENTS (TECHNICAL SAFETY REQUIREMENTS)

4.2.1 Abnormal Reactor Conditions

Section 3.4.1 3.1.1.2 of ref. 16 specifies abnormal conditions for which the reactor must be subcritical. Four cases are identified and reported in Table 13 (reproduced from ref. 16, Table 3.1.1.2-1).

Table 13. Cases for which the reactor must be subcritical

Case	CONTROL ELEMENT Position	Flux Trap Condition
I.	All CONTROL ELEMENTS fully inserted	Optimum void, no target
II.	Four CONTROL ELEMENTS inserted, any one CONTROL ELEMENT fully withdrawn	Optimum void, with target
III.	Three-out-of-four scram from critical, the shim-regulating cylinder immobilized	Optimum void, with target
IV.	Three-out-of-four scram from critical, one shim-safety plate fully withdrawn, the shim-regulating cylinder immobilized	No void, with target

Because the shutdown worth (and fully withdrawn worth) of the reduced-tantalum elements is unchanged from that of the current elements and the current elements meet Cases I and II, the reduced-tantalum elements also meet Cases I and II. For Cases III and IV, the key specification is that the control elements are initially at the symmetric *critical* position. Calculations presented in Sect. 3 of this report show that the differential worth of the reduced-tantalum elements is the same as that of the current elements for corresponding, equivalent-burnup critical configurations.

Given identical core configurations, that is, for a given set of fuel elements, the amount of reactivity that must be added by withdrawal of control and safety elements to achieve criticality is independent of the tantalum content of the elements. Thus, the negative reactivity of the three safety plates scrammed from critical is identical for both the original and lower tantalum concentration safety plates. Because the reactivity added by a postulated void is unchanged, Case III is unaffected by the change in tantalum content.

The reactivity added by a completely withdrawn safety plate is also independent of the tantalum content of the plate. The fully inserted shutdown margin is the same for either plate because it is the europium content that determines this value. Also, the completely withdrawn plate has added an identical amount of reactivity because the aluminum portion of the plates determines the worth of a completely withdrawn plate and this portion is unchanged. Because the plates start at the symmetric critical position

that corresponds to the same reactivity change for either tantalum content plates, the withdrawn plate adds the same amount of reactivity. Thus, Case IV is unaffected by the tantalum content of the plates.

4.2.2 Shutdown Margin Verification

Reference 16 notes (Appendix A, Sect. 3.4.1.2) that,

> it was determined during HFIR startup physics tests that the Case IV shutdown requirement is the more limiting (reactivity accident) hence, it is sufficient (for assuring safety during reactivity accidents) to verify that the Case IV requirement is met. (Case IV is) the scram worth of inserting the three safety plates (when the fourth plate is withdrawn to its full-out position). (It) is determined by their pre-scram critical position. The positive reactivity that may be added by withdrawal of the fourth safety plate is also determined by its initial critical condition. … From (Fig. 20, reproduced from ref. 16), it can be seen that a critical rod position of 16.3 in. or greater ensures adequate Case IV shutdown margin.

Because the progression of the Case IV condition under reduced-tantalum elements will be the same as analyzed for the current elements and because that analysis was confirmed/validated by HFIR startup physics tests, Case IV will remain the more limiting reactivity accident with the reduced-tantalum elements.

The minimum shutdown margin identified in ref. 16 (the technical safety requirements for the HFIR) is derived from the data presented in Fig. 20. The symbols in Fig. 20 correspond to various critical

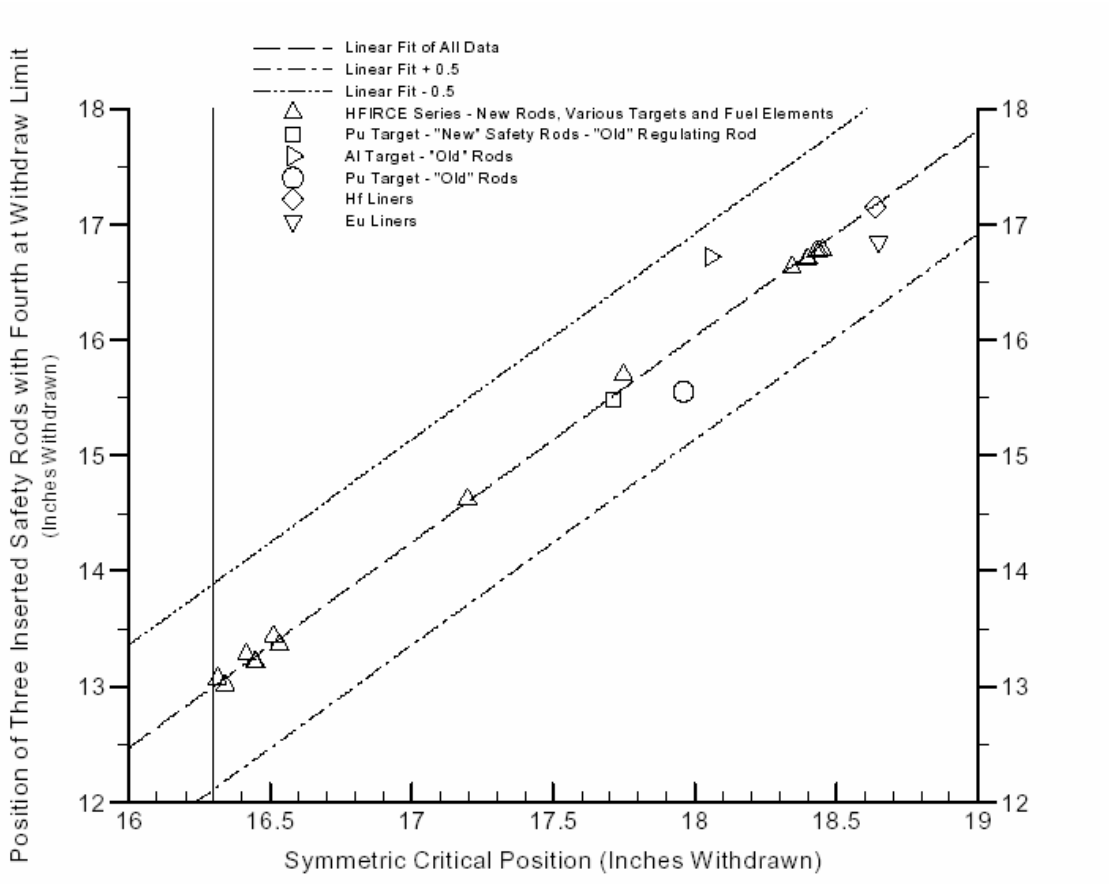

Fig. 20. Case IV subcriticality check (from ref. 16).

configurations achieved during HFIR startup physics tests. Based on the studies presented in Sect. 3 of this report, if each configuration was recreated with the reduced-tantalum-content control and safety elements, each point would shift left and down 1/3 in. Consequently, the "minimum shutdown margin" (value of reactivity worth) associated with control element withdrawal position of 16.3 would be the value associated with the reduced tantalum elements at a withdrawal position of 16.0 in. The value of the minimum shutdown margin is unchanged by the reduced-tantalum-content elements though the location corresponding to that value will be changed (by 1/3 in.).

Section 3.1.1.1 of ref. 16 notes that either the estimated symmetric control element position (ESCCEP) shall be greater than 16.3 in. or an approach-to-critical in a mode 3 configuration can be conducted. Operation of the HFIR with the current target configuration and with reduced-tantalum elements will lead to an ESCCEP of greater than 16.3 in. based on the results of the analyses in Sect. 3 (1/3-in. reduction due to reduced-tantalum content) and the current startup critical positions (18.47 ± 0.4 in. for cycles 388–394). Only operation with the "simulated 300-g Pu target" could be expected to yield a critical control element position less than 16.3 in. Even then, as noted previously, operation is permitted with mode 3 testing of shutdown verification. (The mode 3 testing procedure is proscribed in RRD procedure RTP-2, *Procedure for Determining the Beginning of Cycle ESCCEP of HFIR Control Plates*.)

It is not credible that a request would be made to operate the HFIR in mode 1 (power level of 85 MW) with a "simulated 300-g Pu target." Such a target (or a similar one) would only be used for reactor physics tests. Operation in mode 3 with a "simulated 300 g Pu target" could still be performed with existing procedures but a Case IV test (described in procedure RTP-2) should be performed because the expected symmetric critical withdrawal position would be less than 16.3 in. Using the existing TSR limit of 16.3 in. withdrawn as the minimum symmetric critical control element position that verifies Case IV subcriticality with reduced-tantalum control elements results in a greater shutdown margin than would be expected to be presently required for the reduced-tantalum-content elements. Consequently, no changes are needed to the technical safety requirements for the HFIR.

In Sect. 3.4.1.3.1 of ref. 16, reference is made to the "position of greatest differential worth (i.e., 16.0 in.)." The parenthetical value of 16.00 would likely be slightly different with reduced-tantalum-content elements but could only be achieved with a "simulated 300-g Pu target," and such operation would require a "Case IV" measurement as proscribed in procedure RTP-2.

Reference 14, part 3.1.1.2 states, "Without STRONGLY ABSORBING EXPERIMENTS in the removable beryllium, the Actual Symmetric Critical CONTROL ELEMENT Position shall be 16.3 in. withdrawn or greater." (EMPHASIS is in original document.) With the existing, curium/aluminum rod target, the critical configurations are significantly greater than 16.3 in. If operation with a "simulated 300-g Pu target" were desired, then this proscription would necessitate conducting "Case IV" measurements. The procedure for doing that measurement exists (designated RTP-2).

5. CONCLUSIONS

Regarding nominal, steady-state reactor operation, the impact of the change in the power distribution in the core due to reduced tantalum content was calculated and found to be insignificant. The magnitude and impact of the change in differential control element worth (scram reactivity insertion rate) was calculated, and the differential worth of reduced-tantalum elements vs the current elements from equivalent-burnup *critical* configurations was determined to be unchanged within the accuracy of the computational method and relevant experimental measurements. The change in differential worth at any given control/safety element position due to the reduction in tantalum was found to be independent of element position for values at which the reactor can be made critical during the fuel cycle and the difference in critical positions had a magnitude of –1/3 in., generally independent of position. The magnitude and impact of the change in the shutdown margin (integral rod worth) was assessed, and the analyses that support the USAR were determined to be conservative even for the reduced-tantalum elements.

Because of the invariance of the power distribution under the proposed tantalum change, the proposed reduction in tantalum content would not increase the consequences of an accident previously evaluated in the safety analysis. Because of the invariance of the differential worth *at an equivalent-burnup critical configuration* due to the proposed tantalum change, the proposed reduction in tantalum content would not increase the consequences of a malfunction of equipment important to safety previously evaluated in the safety analyses**.** Because of the invariance of the differential worth *at a critical configuration*, the proposed reduction in tantalum content would not create the possibility of a malfunction of equipment important to safety of a different type other than any previously evaluated in the safety analyses.

The RRD procedure for estimating the symmetric critical control element position (RTP-2) will have to be revised prior to the insertion into the reactor of the reduced-tantalum control and safety elements. No revisions are required to either the technical safety requirements or the USAR for the HFIR.

REFERENCES

1. B. J. Marshall, L. F. Miller, and R. B. Rothrock, *Power Distribution Calculations in the High Flux Isotope Reactor for Various Control Blade Tantalum Loadings*, ORNL/SUB/01-4000000900-1, Oak Ridge National Laboratory, December 2002.

2. R. D. Cheverton and T. M. Sims, *HFIR Core Nuclear Design*, ORNL-4621, Oak Ridge National Laboratory, July 1971.

3. R. T. Primm III, *Reactor Physics Input to the Safety Analysis Report for the High Flux Isotope Reactor*, ORNL/TM-11956, Oak Ridge National Laboratory, March 1992.

4. N. M. Greene, J. W. Arwood, R. Q. Wright, and C. V. Parks, *The LAW Library—A Multigroup Cross-Section Library for Use in Radioactive Waste Analysis Calculations*, ORNL/TM-12370, Oak Ridge National Laboratory, August 1994.

5. S. Goluoglu, R. B. Rothrock, and H. L. Dodds, "Improved Neutronics Calculations of the High-Flux Isotope Reactor," *Trans. Am. Nuc. Soc*., **70**, 349–351 (June 1994).

6. S. Goluoglu and H. L. Dodds, "Improved Neutronics Model of the High-Flux Isotope Reactor," *Nuclear Technology*, **112**, 142–153 (October 1995).

7. W. W. Engle, Jr. and L. R. Williams, *Temperature and Void Reactivity Coefficient Reactivity Calculations for the High Flux Isotope Reactor Safety Analysis Report*, ORNL/TM-12386, Oak Ridge National Laboratory, July 1994.

8. Internal communication from J. T. Thomas, *High Flux Isotope Reactor Critical Experiment No. 3, Part IV, 'Eu_2O_3-Ta-Al Control Cylinder Calibration and Experiments Supporting HFIR Start-up,'* August 16, 1966.

9. J. B. Bullock and H. P. Danforth, *Reactor On-line Computer Control Development at the HFIR, Vol. 1: Objectives, System Design, Operating Experience, and Safety Considerations*, ORNL-TN-3679, Vol. 1, Oak Ridge National Laboratory, October 1972.

10. Howard A. McLain, *HFIR Fuel Element Steady State Heat Transfer Analysis Revised Version*, ORNL-TM-1904, Oak Ridge National Laboratory, December 1967.

11. D. G. Morris and M. W. Wendel, *High Flux Isotope Reactor RELAP5 Input Model*, ORNL/TM-11647, Oak Ridge National Laboratory, January 1993.

12. J. D. Freels, "On RELAP-5-Simulated High Flux Isotope Reactor Reactivity Transients: Code Change and Application," presented at the 1993 RELAP5 International User Seminar, Boston, Massachusetts, July 9, 1993.

13. *SCDAP/RELAP5/MOD2 Code Manual—Volume III: User's Guide and Input Requirements*, NUREG/CR-5273 (EGG-2555), June 1989.

14. *High Flux Isotope Reactor Updated Safety Analysis Report*, April 13, 2001.

15. R. W. Knight and A. E. Richt, "Evaluation of Absorber Materials Performance in HFIR Control Cylinders," *Nuclear Technology*, **15**, 384–390 (September 1972).

16. G. E. Rothenberger, *High Flux Isotope Reactor Technical Safety Requirements*, ORNL/TM-12841, Rev. 5, Oak Ridge National Laboratory, August 30, 2002.

Appendix A. DATASETS

All of the input and output datasets for the cases for which results are presented in this report are stored on the compact disk (CD) and retained under document control according to the procedures of the Research Reactors Division. These data along with the SCALE 4.4a package (distributed on CD from the Radiation Safety Information Computational Center as package CCC-545) and the DOORS 3.2 package (distributed as package CCC-650) should enable any qualified individual to recreate the results presented in this report. For ease of use, the SCALE, GIP, and DORT datasets for the model corresponding to Fig. 3 are included in this appendix. Also included are the datasets used to generate the isotopics for irradiated control/safety elements.

```
=bonami
'hfir ife 4 38% Ta, No target, fuel B for CE-4, 1.25 gB/L, Fig. 7.6
0$$ 84 a4 1
1$$ 1 6 21 0 0 7 t
3$$ 1 6r2 4r3 6r4 4r5
4$$ 13027
   92234 92235 92236 92238 8016 13027
   5010 5011 6012 13027
   13027 4309 63151 63153 73181 73182
   8016 1001 5010 5011
5** 6.03e-2
   1.7012e-5 1.5854e-3 6.8008-6 9.1842e-5 4.5363e-3 4.221e-2
   1.6592e-4 6.7186e-4 2.0951e-4 5.97-2
   6.03e-2 1-10 1-10 1-10 1-10 1-10
   3.309e-2 6.618e-2 1.50554e-5 6.02214e-5
6$$ 5 1 2 3 4 5
7** 0.0635 0.0889 0.14923 0.1651 0.1905 0.254
8** f300.0
10$$ 13027
   92234 92235 92236 92238 8016 130272
   5010 5011 6012 130273
   1302744 4309 63151 63153 73181 73182
   80165 1001 50101 50111
11$$ 1 2 0 2 2 1 t
end
=nitawl
1$$ 0 15 0 0 0 0 0 8 0 0 0 0 t
2$$ 8016 1001
   92234 92235 92236 92238 13027 5010 5011 6012
   63151 63153
   73181 73182
   4309
3** 92234 300.0 1.0 0.02985 0.7066 0.0 1.8779e-5 1.0 26.982 2758.7 1.0
   15.995 3355.5 1.0 1.0
  92235 300.0 1.0 0.02985 0.7066 0.0 1.7503e-3 1.0 26.982 45.816 1.0
   15.995 36.001 1.0 1.0
  92236 300.0 1.0 0.02985 0.7066 0.0 7.5409e-6 1.0 26.982 1.068e4 1.0
   15.995 8356.1 1.0 1.0
  92238 300.0 1.0 0.02985 0.7066 0.0 1.0143e-4 1.0 26.982 790.81 1.0
   15.995 621.24 1.0 1.0
```

```
   63151 300.0 1 0.47625 0.0 0.0 3.38195e-3 1 15.9994 11.867 1 26.982
    8.0426 1 1.0
   63153 300.0 1 0.47625 0.0 0.0 4.12667e-3 1 15.9994 10.866 1 26.982
    7.3647 1 1.0
   73181 300.0 1.0 0.47652 0.0 0.0 1.9025e-2 1.0 26.982 1.3724 1.0
    1.0078 1.5307 1.0 1.0
   73182 300.0 1.0 0.47625 0.0 0.0 1-10 1.0 26.982 1.3724 1.0 1.0078
    1.5307 1.0 1.0
4** f300.0 t
end
=xsdrn
HFIR IFE 4
-1$$ 5000000
1$$ 1 7 30 1 1 5 20 8 5 1 20 100 0 0 0
2$$ -2 9r0
3$$ 1 3r0 5 0 3 5r0
4$$ -1 238 0 -2 3 151 388 -1 0
5** a7 50.8 e t
13$$ 1 6r2 4r3 4r4 5r5
14$$ 13027
   92234 92235 92236 92238 8016 13027
   5010 5011 6012 13027
   8016 1001 5010 5011
   4309 73181 73182 63151 63153
15** 6.03e-2
   1.7012e-5 1.5854e-3 6.8008-6 9.1842e-5 1.667e-2 3.01e-2
   1.6592e-4 6.7186e-4 2.0951e-4 5.97-2
   3.309e-2 6.618e-2 1.50554e-5 6.02214e-5
   1-10 1-10 1-10 1-10 1-10 t
33## f1.0 t
35** 4i 0.0 4i 0.0635 4i 0.08889 4i 0.14923 4i 0.1651 3i 0.1905 0.250
   0.254
36$$ 5r1 5r2 5r3 5r4 5r5 4r6 7
39$$ 4 1 2 3 1 4 5
40$$ 5 5 5 5 5 5 5
51$$ 236i 1 238 t
end
#shell
cp ft03f001 Taife4lib
ln -s Taife4lib ft90f001
end
=xsdrn
HFIR Ta 1D calculations
-1$$ 5000000
0$$ a3 90 e
1$$ 2 27 105 1 0 27 197 8 3 1 20 300 0 0 0
2$$ -2 5r0 0 3r0
3$$ 1 3r0 50 0 3 a9 2 1 e
4$$ 0 44 0 -2 3 26 69 -1 e
5** 1.0e-5 1.0e-5 a4 1.0 a7 50.8 e t
13$$ 2r1 10r2 10r3 10r4 10r5 10r6 10r7 10r8 10r9 9r11 9r12 9r13 9r14
```

9r15 9r16 9r17 9r18 9r19
3r20 5r21 3r22 3r23 3r24
4r25 4r26 5r10 4r27
14$$
8016 1001
92234 92235 92236 92238 8016 13027 5010 5011 6012 1001
92234 92235 92236 92238 8016 13027 5010 5011 6012 1001
92234 92235 92236 92238 8016 13027 5010 5011 6012 1001
92234 92235 92236 92238 8016 13027 5010 5011 6012 1001
92234 92235 92236 92238 8016 13027 5010 5011 6012 1001
92234 92235 92236 92238 8016 13027 5010 5011 6012 1001
92234 92235 92236 92238 8016 13027 5010 5011 6012 1001
92234 92235 92236 92238 8016 13027 5010 5011 6012 1001
92234 92235 92236 92238 13027 8016 1001
5010 5011
92234 92235 92236 92238 13027 8016 1001
5010 5011
92234 92235 92236 92238 13027 8016 1001
5010 5011
92234 92235 92236 92238 13027 8016 1001
5010 5011
92234 92235 92236 92238 13027 8016 1001
5010 5011
92234 92235 92236 92238 13027 8016 1001
5010 5011
92234 92235 92236 92238 13027 8016 1001
5010 5011
92234 92235 92236 92238 13027 8016 1001
5010 5011
13027 1001 8016
73181 73182 13027 1001 8016
13027 1001 8016
13027 1001 8016
13027 1001 8016
4309 13027 8016 1001
4309 13027 8016 1001
1001 8016 13027 5010 5011
63151 63153 13027 8016
15**
3.309-2 6.618-2
2.2070-6 2.0570-4 8.8200-7 1.1920-5 1.667-2 3.01-2
2.29757E-05 9.26807E-05 1.95045E-05 3.33300E-02
2.6930-6 2.5100-4 1.0770-6 1.4540-5 1.667-2 3.01-2
2.09317E-05 8.44007E-05 1.69235E-05 3.33300E-02
3.2520-6 3.0310-4 1.3000-6 1.7560-5 1.667-2 3.01-2
1.86447E-05 7.51407E-05 1.40368E-05 3.33300E-02
4.0400-6 3.7650-4 1.1650-6 2.1810-5 1.667-2 3.01-2
1.53747E-05 6.18907E-05 9.90675E-06 3.33300E-02
4.8070-6 4.4800-4 1.9220-6 2.5960-5 1.667-2 3.01-2

1.21857E-05 4.89807E-05 5.88200E-06 3.33300E-02
4.8770-6 4.5450-4 1.9500-6 2.6330-5 1.667-2 3.01-2
1.19007E-05 4.78207E-05 5.52075E-06 3.33300E-02
4.4750-6 4.1710-4 1.7890-6 2.4170-5 1.667-2 3.01-2
1.36167E-05 5.47707E-05 7.68725E-06 3.33300E-02
3.9890-6 3.7180-4 1.5950-6 2.1540-5 1.667-2 3.01-2
1.55787E-05 6.27207E-05 1.01653E-05 3.33300E-02
4.5280-6 4.2200-4 1.8100-6 2.4450-5 3.01-2 1.667-2 3.333-2
7.5277e-6 3.01107e-5
5.4220-6 5.0530-4 2.1680-6 2.9280-5 3.01-2 1.667-2 3.333-2
7.5277e-6 3.01107e-5
6.3750-6 5.9410-4 2.5490-6 3.4420-5 3.01-2 1.667-2 3.333-2
7.5277e-6 3.01107e-5
7.2400-6 6.7470-4 2.8940-6 3.9090-5 3.01-2 1.667-2 3.333-2
7.5277e-6 3.01107e-5
6.975-6 6.50-4 2.27-6 3.066-5 3.01-2 1.667-2 3.333-2
7.5277e-6 3.01107e-5
5.6780-6 5.2920-4 2.2700-6 3.0660-5 3.01-2 1.667-2 3.333-2
7.5277e-6 3.01107e-5
4.4480-6 4.1450-4 1.7780-6 2.4020-5 3.01-2 1.667-2 3.333-2
7.5277e-6 3.01107e-5
3.6340-6 3.3870-4 1.4530-6 1.9620-5 3.01-2 1.667-2 3.333-2
7.5277e-6 3.01107e-5
2.8950-6 2.6980-4 1.1570-6 1.5630-5 3.01-2 1.667-2 3.333-2
7.5277e-6 3.01107e-5
4.6012e-2 1.58012e-2 7.90058e-3
1.9025e-2 1-10 3.0635e-2 2r1.0e-20
1.96891e-2 4.48968e-2 2.24484e-2
5.7401e-2 1.5703e-3 3.1407e-3
2.47544e-2 3.92980e-2 1.9649e-2
1.167-1 5.52-4 1.64e-3 3.28e-3
1.208-1 5.6-4 4.97-4 9.94-4
2.75-2 1.375-2 3.534-2 6.21097e-6 2.48439e-5
3.83195e-3 4.12667e-3 3.09830e-2 1.19379e-2
t t
33## f1.0 t
35** 2i 0.0 2i 7.14 2i 7.5 2i 8.0 2i 8.5 2i 9.5 2i 10.5 2i 11.5
2i 12.0 2i 12.6 2i 15.15 2i 15.5 2i 16.0 2i 16.5 2i 17.5
2i 18.5 2i 19.5 2i 20.0 2i 20.5 2i 21.0
4i22.1037 22.58 23.0664 23.5426 8i24.15
20i33.0 6i54.0 54.635
36$$ 3r1 3r2 3r3 3r4 3r5 3r6 3r7 3r8 3r9 3r10 3r11 3r12 3r13 3r14
3r15 3r16 3r17 3r18 3r19
3r20 5r21 22 23 24 9r25 21r26 7r27
39$$ 25i1 27
49$$
92235 92238
50$$
18 18
51$$ 7r1 2 3 2r4 5 6 7 2r8 8r9 14r10 6r11 10r12 13 7r14 11r15 12r16
30r17 16r18 2r19 6r20 3r21 6r22 14r23 27r24 10r25 5r26 27 28 29

```
   2r30 31 32 33 2r34 2r35 3r36 2r37 38 39 40 41 42 3r43 9r44 t
end
=shell
cp ft03f001 38Ta100_ampx
ln -s 38Ta100_ampx ft91f001
end
=alpo
0$$ 20 91
1$$ 1 3 26 69 3 e t
2$$ 91 0 t t
end
=shell
cp ft20f001 /home/rtp/Ta/crits/Fig7.6/38%Ta/fort.9
end
=gip
/gip for Fig. 7.6
1$$ 44 3 26 69 219 0 788 924 0 3 2 2 2 e t
13$$ 786i1 788
10$$ 2r-789 10r-793 10r-797 10r-801 10r-805 10r-809
10r-813 10r-817 10r-821 9r-825 9r-829 9r-833 9r-837
 9r-841 9r-845 9r-849 9r-853 9r-857
3r-861 5r-865 3r-869 3r-873 3r-877 4r-881 4r-885
5r-889 4r-893 2r-897 3r-901 2r-905 3r-909 5r-913
5r-917 2r-921
11$$
/ DORT mixture IDs, definition; Pg. 111, ORNL-4621
/   with modification to explicitly model control
/   and safety elements
/
/ Target for Fig. 7.6
/
/ GIP ids for mixture / comment (Fig. A.8 regions)
 465 357 / target 1
 577 721 645 185 361 253 9 81 153 469 / inner 4
 581 725 649 189 365 257 13 85 157 473 / inner 5
 585 729 653 193 369 261 17 89 161 477 / inner 6
 589 733 657 197 373 265 21 93 165 481 / inner 7
 593 737 661 201 377 269 25 97 169 485 / inner 8
 597 741 665 205 381 273 29 101 173 489 / inner 9
 601 745 669 209 385 277 33 105 177 493 / inner 10
 605 749 673 213 389 281 37 109 181 497 / inner 11
 609 753 677 217 289 397 505 45 117 / outer 13
 613 757 681 221 293 401 509 49 121 / outer 14
 617 761 685 225 297 405 513 53 125 / outer 15
 621 765 689 229 301 409 517 57 129 / outer 16
 625 769 693 233 305 413 521 61 133 / outer 17
 629 773 697 237 309 417 525 65 137 / outer 18
 633 777 701 241 313 421 529 69 141 / outer 19
 637 781 705 245 317 425 533 73 145 / outer 20
 641 785 709 249 321 429 537 77 149 / outer 21
 325 541 433 / wall + water + clad = 22
```

573 717 329 545 437 / Ta = 23-I or O, partial
333 549 441 / clad + water + clad = part of 22, 23, 24
337 553 445 / Al portion of ctl/safety ele. = part of 22
341 557 449 / clad + water + wall of Be = part of 22, 23, 24
1 345 453 561 / inner ref 25
5 349 457 565 / outer ref 26
501 393 285 41 113 / side plate and water gap between ele. 12
569 713 353 461 / Eu = 24-I or O, partial
357 465 / gap 2
361 469 253 / side plate 3 (O, H, Al)
457 565 / Water (Reg 27)
361 469 253 / Water and Al (Reg 28)
373 481 265 21 93 / Water and Al (Reg 29)
409 517 301 57 129 / Water and Al (Reg 30)
457 565 / Water (Reg 31)
12**
3.309-2 6.618-2
2.2070-6 2.0570-4 8.8200-7 1.1920-5 1.667-2 3.01-2
2.29757-05 9.26807-05 1.95045-05 3.33300-02
2.6930-6 2.5100-4 1.0770-6 1.4540-5 1.667-2 3.01-2
2.09317-05 8.44007-05 1.69235-05 3.33300-02
3.2520-6 3.0310-4 1.3000-6 1.7560-5 1.667-2 3.01-2
1.86447-05 7.51407-05 1.40368-05 3.33300-02
4.0400-6 3.7650-4 1.1650-6 2.1810-5 1.667-2 3.01-2
1.53747-05 6.18907-05 9.90675-06 3.33300-02
4.8070-6 4.4800-4 1.9220-6 2.5960-5 1.667-2 3.01-2
1.21857-05 4.89807-05 5.88200-06 3.33300-02
4.8770-6 4.5450-4 1.9500-6 2.6330-5 1.667-2 3.01-2
1.19007-05 4.78207-05 5.52075-06 3.33300-02
4.4750-6 4.1710-4 1.7890-6 2.4170-5 1.667-2 3.01-2
1.36167-05 5.47707-05 7.68725-06 3.33300-02
3.9890-6 3.7180-4 1.5950-6 2.1540-5 1.667-2 3.01-2
1.55787-05 6.27207-05 1.01653-05 3.33300-02
4.5280-6 4.2200-4 1.8100-6 2.4450-5 3.01-2 1.667-2 3.333-2
7.5277e-6 3.01107e-5
5.4220-6 5.0530-4 2.1680-6 2.9280-5 3.01-2 1.667-2 3.333-2
7.5277e-6 3.01107e-5
6.3750-6 5.9410-4 2.5490-6 3.4420-5 3.01-2 1.667-2 3.333-2
7.5277e-6 3.01107e-5
7.2400-6 6.7470-4 2.8940-6 3.9090-5 3.01-2 1.667-2 3.333-2
7.5277e-6 3.01107e-5
6.975-6 6.50-4 2.27-6 3.066-5 3.01-2 1.667-2 3.333-2
7.5277e-6 3.01107e-5
5.6780-6 5.2920-4 2.2700-6 3.0660-5 3.01-2 1.667-2 3.333-2
7.5277e-6 3.01107e-5
4.4480-6 4.1450-4 1.7780-6 2.4020-5 3.01-2 1.667-2 3.333-2
7.5277e-6 3.01107e-5
3.6340-6 3.3870-4 1.4530-6 1.9620-5 3.01-2 1.667-2 3.333-2
7.5277e-6 3.01107e-5
2.8950-6 2.6980-4 1.1570-6 1.5630-5 3.01-2 1.667-2 3.333-2
7.5277e-6 3.01107e-5

```
4.6012e-2 1.58012e-2 7.90058e-3
1.9025e-2 1-10 3.0635e-2 2r1.0e-20
1.96891e-2 4.48968e-2 2.24484e-2
5.7401e-2 1.5703e-3 3.1407e-3
2.47544e-2 3.92980e-2 1.9649e-2
1.167-1 5.52-4 1.64e-3 3.28e-3
1.208-1 5.6-4 4.97-4 9.94-4
2.75-2 1.375-2 3.534-2 6.21097e-6 2.48439e-5
3.83195e-3 4.12667e-3 3.09830e-2 1.19379e-2
/ Start of description of extra regions
3.309-2 6.618-2
5.37-3 1.074-2 4.8-2
3.333-2 6.666-2
1.92-2 3.83-2 2.36-2
1.667-2 3.333-2 3.01-2 7.5277e-6 3.01107e-5
1.667-2 3.333-2 3.01-2 7.5277e-6 3.01107e-5
3.333-2 6.666-2
t
=end
=dort
HFIR RZ Core Model - ORNL-4621, Fig. 7.6, blades at 24.3 in, 38%
61$$ 0 0 8 e
62$$ 0 3 34 102 95 44 3 26 69 0 0 0 136 0 48 1 3 0 0 0
   200 20 0 0 1 2 0 0 3 0 0 0 0 0 1 34 0 1 1 0 0 0 0 0 0
   0 1 1 1 1 4 50 0 0 5 0 0 0 0 0 0 -1 5000 0 0 4 -1 0 0 0 e
63** 2000 a3 1.0e-5 a6 1.0e-5 e t
t
82*
 0 -30861- 5 0 -21822- 5 0 +21822- 5 0 -61721- 5 0 -57735- 5 0 -21822- 5
 0 +21822- 5 0 +57735- 5 0 -81650- 5 0 -78680- 5 0 -57735- 5 0 -21822- 5
 0 +21822- 5 0 +57735- 5 0 +78680- 5 0 -97590- 5 0 -95119- 5 0 -78680- 5
 0 -57735- 5 0 -21822- 5 0 +21822- 5 0 +57735- 5 0 +78680- 5 0 +95119- 5
 0 -30861- 5 0 -21822- 5 0 +21822- 5 0 -61721- 5 0 -57735- 5 0 -21822- 5
 0 +21822- 5 0 +57735- 5 0 -81650- 5 0 -78680- 5 0 -57735- 5 0 -21822- 5
 0 +21822- 5 0 +57735- 5 0 +78680- 5 0 -97590- 5 0 -95119- 5 0 -78680- 5
 0 -57735- 5 0 -21822- 5 0 +21822- 5 0 +57735- 5 0 +78680- 5 0 +95119- 5
83*
 3r-95119- 5 5r-78680- 5 7r-57735- 5 9r-21822- 5 3r+95119- 5 5r+78680- 5
 7r+57735- 5 9r+21822- 5
81*
 0 + 0+ 0 2r+30247- 6 0 + 0+ 0 0 +22685- 6 2r+22685- 6 0 +22685- 6
 0 + 0+ 0 0 +22685- 6 0 +23148- 6 2r+22685- 6 0 +23148- 6 0 +22685- 6
 0 + 0+ 0 0 +30247- 6 0 +22685- 6 0 +22685- 6 2r+30247- 6 0 +22685- 6
 0 +22685- 6 0 +30247- 6 0 + 0+ 0 2r+30247- 6 0 + 0+ 0 0 +22685- 6
 2r+22685- 6 0 +22685- 6 0 + 0+ 0 0 +22685- 6 0 +23148- 6 2r+22685- 6
 0 +23148- 6 0 +22685- 6 0 + 0+ 0 0 +30247- 6 0 +22685- 6 0 +22685- 6
 2r+30247- 6 0 +22685- 6 0 +22685- 6 0 +30247- 6
t
1** 5.09e-3 1.40e-2 4.39e-2 1.53e-1 8.52e-2 2.41e-2 1.15e-1
   1.27e-1 1.65e-1 1.73e-1 8.29e-2 1.18e-2 7.61e-4 9.05e-4
   6.72e-5 5.28e-6 3.71e-7 5.89e-8 3.81e-9 3.71e-9 1.93e-9
```

```
   2.29e-9 1.26e-9 6.02e-10 2.25e-10 1.07e-10 1.04e-11 1e-11
   9.68e-12 1.82e-11 8.53e-12 8.12e-12 7.68e-12 1.39e-11
   1.18e-11 5.82e-12 3.26e-12 1.41e-12 1.25e-12 5.21e-13
   1.34e-12 1.56e-13 2.16e-13 7.30e-14
2**
5i-65.0
4i -40.0
   -31.242
6i -30.48
2i -25.4 2i -25.0 -23.0 4i-21.0 2i-19.0
   4i-18.542
-17.0 -15.0 -13.0 -11.0 -9.0 -7.0 -5.0 -3.0 -1.0
1.0 3.0 5.0 7.0 9.0 11.0 13.0 15.0 4i17.0
   2i18.542
4i19.0 21.0 2i23.0 2i25.0 6i25.4
30.48
   4i31.242
5i40.0
65.0
4**
4i 0.0
2i 5.0
2i 6.4
2i 7.14
2i 7.5
8.0 8.5 9.0 9.5 10.0 10.5 11.0 11.5 2i 12.0
3i 12.6
2i 15.15
2i 15.5
16 16.5 17.0 17.5 18.0 18.5 19.0 19.5
4i 20.0
4i 20.5
2i 21.0
4i22.1037 22.58 4i23.0664 23.5426 13i24.15
10i 33.0
5i 54.0
79.0
5** 2e7 8.1873e6 6.434e6 4.8e6 3e6 2.479e6 2.354e6 1.85e6 1.4e6
   9e5 4e5 1e5 2.5e4 1.7e4 3e3 5.5e2 1e2 3e1 1e1 8.1 6.0 4.75
   3.0 1.77 1.0 6.25e-1 4e-1 3.75e-1 3.5e-1 3.25e-1 2.75e-1
   2.5e-1 2.25e-1 2e-1 1.5e-1 1e-1 7e-2 5e-2 4e-2 3e-2 2.53e-2
   1e-2 7.5e-3 3e-3 1e-5 0
/ DORT x-sect,  Comment  Table A.6, ORNL-4621 region #
/ Mat zone Mat #
/ 1       1       target          1
/ 2       5       inner fuel      4
/ 3       9       inner fuel      5
/ 4       13      inner fuel      6
/ 5       17      inner fuel      7
/ 6       21      inner fuel      8
/ 7       25      inner fuel      9
```

```
/ 8      29      inner fuel      10
/ 9      33      inner fuel      11
/ 10     37      outer fuel      13
/ 11     41      outer fuel      14
/ 12     45      outer fuel      15
/ 13     49      outer fuel      16
/ 14     53      outer fuel      17
/ 15     57      outer fuel      18
/ 16     61      outer fuel      19
/ 17     65      outer fuel      20
/ 18     69      outer fuel      21
/ 19     73      wall + water + clad = 22
/ 20     77      Ta = 23-I or O, partial
/ 21     81      clad + water + clad = part of 22, 23, 24
/ 22     85      Al portion of ctl, sfty plates = part of 22
/ 23     89      clad + water + wall of Be = part of 22, 23, 24
/ 24     93      inner ref 25
/ 25     97      outer ref 26
/ 26     101     side plate and water gap between ele. 12
/ 27     105     Eu = 24-I or O, partial
/ 28     109     gap 2
/ 29     113     side plate 3 (O, H, Al)
/ 30     117     Water (Reg 27)
/ 31     121     Water and Al (Reg 28)
/ 32     125     Water and Al (Reg 29)
/ 33     129     Water and Al (Reg 30)
/ 34     133     Water (Reg 31)
8$$
5r34 3r34 3r29 17r34          4r34
 24r34          3r19 5r27 21 5r22 23 14r34 11r34 6r34
   5q102
5r31 3r34 3r29 17r34          4r34
 24r34          3r19 5r27 21 5r22 23 14r34 11r34 6r34
   4q102
5r31 3r34 3r29 17r32          4r26
 24r33          3r19 5r27 21 5r22 23 14r24 11r25 6r30

5r31 3r34 3r29 17r32          4r26
 24r33          3r19 5r20 21 5r22 23 14r24 11r25 6r30
   6q102
5r1 3r28 3r29 3r2 3r3 4 5 5 6 6 7 7 8 3r9 4r26
3r10 3r11 12 13 13 14 14 15 15 16 5r17 5r18
          3r19 5r20 21 5r22 23 14r24 11r25 6r30
   14q102
5r1 3r28 3r29 3r2 3r3 4 5 5 6 6 7 7 8 3r9 4r26
3r10 3r11 12 13 13 14 14 15 15 16 5r17 5r18
          3r19 5r22 21 5r22 23 14r24 11r25 6r30
   26q102
5r1 3r28 3r29 3r2 3r3 4 5 5 6 6 7 7 8 3r9 4r26
3r10 3r11 12 13 13 14 14 15 15 16 5r17 5r18
          3r19 5r22 21 5r20 23 14r24 11r25 6r30
```

```
   14q102
5r31 3r34 3r29 17r32              4r26
 24r33             3r19 5r22 21 5r20 23 14r24 11r25 6r30
   6q102
5r31 3r34 3r29 17r32              4r26
 24r33             3r19 5r22 21 5r27 23 14r24 11r25 6r30

5r31 3r34 3r29 17r34              4r34
 24r34             3r19 5r22 21 5r27 23 14r34 11r34 6r34
   4q102
5r34 3r34 3r29 17r34              4r34
 24r34             3r19 5r22 21 5r27 23 14r34 11r34 6r34
   5q102
9$$ 32i1 133
26$$ 2
t
93** f 1.0 t
94** f 1.0 t
95** f 1.0 t
=end
```

The following dataset was used to generate isotopics for the tantalum region of the control elements after irradiation to 100,000 MWD.

```
=bonami
0$$ 84 a4 1
1$$ 1 6 20 0 0 7 t
3$$ 1 6r2 4r3 7r4 2r5
4$$ 13027
    92234 92235 92236 92238 8016 13027
    5010 5011 6012 13027
    13027 4309 63151 63153 73181 73182 47109
    8016 1001
5** 6.03e-2
    1.7012e-5 1.5854e-3 6.8008-6 9.1842e-5 4.5363e-3 4.221e-2
    1.6592e-4 6.7186e-4 2.0951e-4 5.97-2
    6.03e-2 1-10 1-10 1-10 1-10 1-10 1.0e-20
    3.309e-2 6.618e-2
6$$ 5 1 2 3 4 5
7** 0.0635 0.0889 0.14923 0.1651 0.1905 0.254
8** f300.0
10$$ 13027
     92234 92235 92236 92238 8016 130272
     5010 5011 6012 130273
     1302744 4309 63151 63153 73181 73182 47109
     80165 1001
11$$ 1 2 0 2 2 1 t

end
=nitawl
1$$ 0 16 0 0 0 0 0 8 0 0 0 0 t
2$$ 8016 1001
```

```
    92234 92235 92236 92238 13027 5010 5011 6012
    63151 63153
    73181 73182
    4309 47109
3** 92234 300.0 1.0 0.02985 0.7066 0.0 1.8779e-5 1.0 26.982 2758.7 1.0
     15.995 3355.5 1.0 1.0
    92235 300.0 1.0 0.02985 0.7066 0.0 1.7503e-3 1.0 26.982 45.816 1.0
     15.995 36.001 1.0 1.0
    92236 300.0 1.0 0.02985 0.7066 0.0 7.5409e-6 1.0 26.982 1.068e4 1.0
     15.995 8356.1 1.0 1.0
    92238 300.0 1.0 0.02985 0.7066 0.0 1.0143e-4 1.0 26.982 790.81 1.0
     15.995 621.24 1.0 1.0
    63151 300.0 1 0.47625 0.0 0.0 3.38195e-3 1 15.9994 11.867 1 26.982
     8.0426 1 1.0
    63153 300.0 1 0.47625 0.0 0.0 4.12667e-3 1 15.9994 10.866 1 26.982
     7.3647 1 1.0
    73181 300.0 1.0 0.47652 0.0 0.0 1.9025e-2 1.0 26.982 1.3724 1.0
     1.0078 1.5307 1.0 1.0
    73182 300.0 1.0 0.47625 0.0 0.0 1-10 1.0 26.982 1.3724 1.0 1.0078
     1.5307 1.0 1.0
4** f300.0 t

end
=xsdrn
HFIR Ta 1D calculations
-1$$ 5000000
1$$ 2 27 105 1 0 27 183 8 3 1 20 300 0 0 0
2$$ -2 5r0 0 3r0
3$$ 1 3r0 50 0 3 a9 2 1 e
4$$ 1 44 0 -2 3 26 69 -1 e
5** 1.0e-5 1.0e-5 a4 1.0 a7 50.8  e t
13$$ 8r1 10r2 10r3 10r4 10r5 10r6 10r7 10r8 10r9 7r11 7r12 7r13 7r14
     7r15 7r16 7r17 7r18 7r19 3r20 5r21 3r22 3r23 3r24
     4r25 4r26 3r10 4r27
14$$
1001 8016 13027 5010 5011 47109 92235 92238
     92234 92235 92236 92238 8016 13027 5010 5011 6012 1001
     92234 92235 92236 92238 8016 13027 5010 5011 6012 1001
     92234 92235 92236 92238 8016 13027 5010 5011 6012 1001
     92234 92235 92236 92238 8016 13027 5010 5011 6012 1001
     92234 92235 92236 92238 8016 13027 5010 5011 6012 1001
     92234 92235 92236 92238 8016 13027 5010 5011 6012 1001
     92234 92235 92236 92238 8016 13027 5010 5011 6012 1001
     92234 92235 92236 92238 8016 13027 5010 5011 6012 1001
     92234 92235 92236 92238 13027 8016 1001
     92234 92235 92236 92238 13027 8016 1001
     92234 92235 92236 92238 13027 8016 1001
     92234 92235 92236 92238 13027 8016 1001
     92234 92235 92236 92238 13027 8016 1001
     92234 92235 92236 92238 13027 8016 1001
     92234 92235 92236 92238 13027 8016 1001
     92234 92235 92236 92238 13027 8016 1001
13027 1001 8016
     73181 73182 13027 1001 8016
13027 1001 8016
13027 1001 8016
```

```
13027 1001 8016
     4309 13027 8016 1001
     4309 13027 8016 1001
     1001 8016 13027
     63151 1001 13027 8016
15**
3.83e-2 1.92e-2 2.36e-2 1.184e-6 4.8e-6 7.32e-5 5.361e-6
8.25e-5
     2.2070-6 2.0570-4 8.8200-7 1.1920-5 1.667-2 3.01-2
  1.54480E-05  6.25700E-05  1.95045E-05  3.33300E-02
     2.6930-6 2.5100-4 1.0770-6 1.4540-5 1.667-2 3.01-2
  1.34040E-05  5.42900E-05  1.69235E-05  3.33300E-02
     3.2520-6 3.0310-4 1.3000-6 1.7560-5 1.667-2 3.01-2
  1.11170E-05  4.50300E-05  1.40368E-05  3.33300E-02
     4.0400-6 3.7650-4 1.1650-6 2.1810-5 1.667-2 3.01-2
  7.84700E-06  3.17800E-05  9.90675E-06  3.33300E-02
     4.8070-6 4.4800-4 1.9220-6 2.5960-5 1.667-2 3.01-2
  4.65800E-06  1.88700E-05  5.88200E-06  3.33300E-02
     4.8770-6 4.5450-4 1.9500-6 2.6330-5 1.667-2 3.01-2
  4.37300E-06  1.77100E-05  5.52075E-06  3.33300E-02
     4.4750-6 4.1710-4 1.7890-6 2.4170-5 1.667-2 3.01-2
  6.08900E-06  2.46600E-05  7.68725E-06  3.33300E-02
     3.9890-6 3.7180-4 1.5950-6 2.1540-5 1.667-2 3.01-2
  8.05100E-06  3.26100E-05  1.01653E-05  3.33300E-02
     4.5280-6 4.2200-4 1.8100-6 2.4450-5 3.01-2 1.667-2 3.333-2
     5.4220-6 5.0530-4 2.1680-6 2.9280-5 3.01-2 1.667-2 3.333-2
     6.3750-6 5.9410-4 2.5490-6 3.4420-5 3.01-2 1.667-2 3.333-2
     7.2400-6 6.7470-4 2.8940-6 3.9090-5 3.01-2 1.667-2 3.333-2
     6.975-6 6.50-4 2.27-6 3.066-5 3.01-2 1.667-2 3.333-2
     5.6780-6 5.2920-4 2.2700-6 3.0660-5 3.01-2 1.667-2 3.333-2
     4.4480-6 4.1450-4 1.7780-6 2.4020-5 3.01-2 1.667-2 3.333-2
     3.6340-6 3.3870-4 1.4530-6 1.9620-5 3.01-2 1.667-2 3.333-2
     2.8950-6 2.6980-4 1.1570-6 1.5630-5 3.01-2 1.667-2 3.333-2
4.6012e-2 1.58012e-2 7.90058e-3
1.9025e-2 1-10 3.0635e-2 2r1.0e-20
1.96891e-2 4.48968e-2 2.24484e-2
5.7401e-2 1.5703e-3 3.1407e-3
2.47544e-2 3.92980e-2 1.9649e-2
1.167-1 5.52-4 1.64e-3 3.28e-3
1.208-1 5.6-4  4.97-4  9.94-4
2.75-2 1.375-2 3.534-2
3.38195e-3 4.12667e-3 3.09830e-2 1.19379e-2
t
33## f1.0 t
35** 2i 0.0 2i 7.14 2i 7.5 2i 8.0 2i 8.5 2i 9.5 2i 10.5 2i 11.5
     2i 12.0 2i 12.6 2i 15.15 2i 15.5 2i 16.0 2i 16.5 2i 17.5
     2i 18.5 2i 19.5 2i 20.0 2i 20.5 2i 21.0
     4i22.1037 22.58 23.0664 23.5426 8i24.15
     20i33.0 6i54.0 54.635
36$$ 3r1 3r2 3r3 3r4 3r5 3r6 3r7 3r8 3r9 3r10 3r11 3r12 3r13 3r14
     3r15 3r16 3r17 3r18 3r19 3r20 5r21 22 23 24 9r25 21r26 7r27
39$$ 25i1 27
49$$
92235 92238
50$$
18 18
51$$ 7r1 2 3 2r4 5 6 7 2r8 8r9 14r10 6r11 10r12 13 7r14 11r15 12r16
```

```
     30r17 16r18 2r19 6r20 3r21 6r22 14r23 27r24 10r25 5r26 27 28 29
     2r30 31 32 33 2r34 2r35 3r36 2r37 38 39 40 41 42 3r43 9r44 t
end
=couple

0$$ a3 3 22 e
1$$ a12 731810 a17 18 17 9 e t
done
end
=origens
0$$ a4 32 a11 86 e
1$$ 1
t
Irradition of Ta portion of control element
3$$ 32 a3 1 a16 2 e
5$$ 2
t
35$$ 0
4t
56$$ 12 12 1 1 a13 1 4 2 a18 1 e
5t
1 gram of Ta
59** f 1.9665e+14
60** 1 2 4 8 16 32 64 128 256 571.94 1024 1176
66$$ 0 0 0 2 f 0.0
73$$
731810
74**
1.0
75$$ f4
t
56$$ 0 1 a10 12 e
t
60** 0.001
65$$ f0 a5 1 a8 1 a11 1 a14 1 e
t
56$$ f0 t
end
```

The following dataset was used to generate isotopics for the europium region of the control elements after irradiation to 100,000 MWD.

```
=bonami
0$$ 84 a4 1
1$$ 1 6 20 0 0 7 t
3$$ 1 6r2 4r3 7r4 2r5
4$$ 13027
    92234 92235 92236 92238 8016 13027
    5010 5011 6012 13027
    13027 4309 63151 63153 73181 73182 47109
    8016 1001
5** 6.03e-2
    1.7012e-5 1.5854e-3 6.8008-6 9.1842e-5 4.5363e-3 4.221e-2
    1.6592e-4 6.7186e-4 2.0951e-4 5.97-2
    6.03e-2 1-10 1-10 1-10 1-10 1-10 1.0e-20
```

```
    3.309e-2 6.618e-2
6$$ 5 1 2 3 4 5
7** 0.0635 0.0889 0.14923 0.1651 0.1905 0.254
8** f300.0
10$$ 13027
     92234 92235 92236 92238 8016 130272
     5010 5011 6012 130273
     1302744 4309 63151 63153 73181 73182 47109
     80165 1001
11$$ 1 2 0 2 2 1 t

end
=nitawl
1$$ 0 16 0 0 0 0 0 8 0 0 0 0 t
2$$ 8016 1001
    92234 92235 92236 92238 13027 5010 5011 6012
    63151 63153
    73181 73182
    4309 47109
3** 92234 300.0 1.0 0.02985 0.7066 0.0 1.8779e-5 1.0 26.982 2758.7 1.0
     15.995 3355.5 1.0 1.0
    92235 300.0 1.0 0.02985 0.7066 0.0 1.7503e-3 1.0 26.982 45.816 1.0
     15.995 36.001 1.0 1.0
    92236 300.0 1.0 0.02985 0.7066 0.0 7.5409e-6 1.0 26.982 1.068e4 1.0
     15.995 8356.1 1.0 1.0
    92238 300.0 1.0 0.02985 0.7066 0.0 1.0143e-4 1.0 26.982 790.81 1.0
     15.995 621.24 1.0 1.0
    63151 300.0 1 0.47625 0.0 0.0 3.38195e-3 1 15.9994 11.867 1 26.982
     8.0426 1 1.0
    63153 300.0 1 0.47625 0.0 0.0 4.12667e-3 1 15.9994 10.866 1 26.982
     7.3647 1 1.0
    73181 300.0 1.0 0.47652 0.0 0.0 1.9025e-2 1.0 26.982 1.3724 1.0
     1.0078 1.5307 1.0 1.0
    73182 300.0 1.0 0.47625 0.0 0.0 1-10 1.0 26.982 1.3724 1.0 1.0078
     1.5307 1.0 1.0
4** f300.0 t

end
=xsdrn
HFIR Eu 1D calculations
-1$$ 5000000
1$$ 2 27 105 1 0 27 183 8 3 1 20 300 0 0 0
2$$ -2 5r0 0 3r0
3$$ 1 3r0 50 0 3 a9 2 1 e
4$$ 1 44 0 -2 3 26 69 -1 e
5** 1.0e-5 1.0e-5 a4 1.0 a7 50.8  e t
13$$ 8r1 10r2 10r3 10r4 10r5 10r6 10r7 10r8 10r9 7r11 7r12 7r13 7r14
     7r15 7r16 7r17 7r18 7r19 3r20 5r27 3r22 3r23 3r24
     4r25 4r26 3r10 4r21
14$$
1001 8016 13027 5010 5011 47109 92235 92238
     92234 92235 92236 92238 8016 13027 5010 5011 6012 1001
     92234 92235 92236 92238 8016 13027 5010 5011 6012 1001
     92234 92235 92236 92238 8016 13027 5010 5011 6012 1001
     92234 92235 92236 92238 8016 13027 5010 5011 6012 1001
     92234 92235 92236 92238 8016 13027 5010 5011 6012 1001
     92234 92235 92236 92238 8016 13027 5010 5011 6012 1001
```

```
     92234 92235 92236 92238 8016 13027 5010 5011 6012 1001
     92234 92235 92236 92238 8016 13027 5010 5011 6012 1001
     92234 92235 92236 92238 13027 8016 1001
     92234 92235 92236 92238 13027 8016 1001
     92234 92235 92236 92238 13027 8016 1001
     92234 92235 92236 92238 13027 8016 1001
     92234 92235 92236 92238 13027 8016 1001
     92234 92235 92236 92238 13027 8016 1001
     92234 92235 92236 92238 13027 8016 1001
     92234 92235 92236 92238 13027 8016 1001
     92234 92235 92236 92238 13027 8016 1001
13027 1001 8016
     73181 73182 13027 1001 8016
13027 1001 8016
13027 1001 8016
13027 1001 8016
     4309 13027 8016 1001
     4309 13027 8016 1001
     1001 8016 13027
     63151 1001 13027 8016
15**
3.83e-2 1.92e-2 2.36e-2 1.184e-6 4.8e-6 7.32e-5 5.361e-6
8.25e-5
     2.2070-6 2.0570-4 8.8200-7 1.1920-5 1.667-2 3.01-2
  1.54480E-05  6.25700E-05  1.95045E-05  3.33300E-02
     2.6930-6 2.5100-4 1.0770-6 1.4540-5 1.667-2 3.01-2
  1.34040E-05  5.42900E-05  1.69235E-05  3.33300E-02
     3.2520-6 3.0310-4 1.3000-6 1.7560-5 1.667-2 3.01-2
  1.11170E-05  4.50300E-05  1.40368E-05  3.33300E-02
     4.0400-6 3.7650-4 1.1650-6 2.1810-5 1.667-2 3.01-2
  7.84700E-06  3.17800E-05  9.90675E-06  3.33300E-02
     4.8070-6 4.4800-4 1.9220-6 2.5960-5 1.667-2 3.01-2
  4.65800E-06  1.88700E-05  5.88200E-06  3.33300E-02
     4.8770-6 4.5450-4 1.9500-6 2.6330-5 1.667-2 3.01-2
  4.37300E-06  1.77100E-05  5.52075E-06  3.33300E-02
     4.4750-6 4.1710-4 1.7890-6 2.4170-5 1.667-2 3.01-2
  6.08900E-06  2.46600E-05  7.68725E-06  3.33300E-02
     3.9890-6 3.7180-4 1.5950-6 2.1540-5 1.667-2 3.01-2
  8.05100E-06  3.26100E-05  1.01653E-05  3.33300E-02
     4.5280-6 4.2200-4 1.8100-6 2.4450-5 3.01-2 1.667-2 3.333-2
     5.4220-6 5.0530-4 2.1680-6 2.9280-5 3.01-2 1.667-2 3.333-2
     6.3750-6 5.9410-4 2.5490-6 3.4420-5 3.01-2 1.667-2 3.333-2
     7.2400-6 6.7470-4 2.8940-6 3.9090-5 3.01-2 1.667-2 3.333-2
     6.975-6 6.50-4 2.27-6 3.066-5 3.01-2 1.667-2 3.333-2
     5.6780-6 5.2920-4 2.2700-6 3.0660-5 3.01-2 1.667-2 3.333-2
     4.4480-6 4.1450-4 1.7780-6 2.4020-5 3.01-2 1.667-2 3.333-2
     3.6340-6 3.3870-4 1.4530-6 1.9620-5 3.01-2 1.667-2 3.333-2
     2.8950-6 2.6980-4 1.1570-6 1.5630-5 3.01-2 1.667-2 3.333-2
4.6012e-2 1.58012e-2 7.90058e-3
1.9025e-2 1-10 3.0635e-2 2r1.0e-20
1.96891e-2 4.48968e-2 2.24484e-2
5.7401e-2 1.5703e-3 3.1407e-3
2.47544e-2 3.92980e-2 1.9649e-2
1.167-1 5.52-4 1.64e-3 3.28e-3
1.208-1 5.6-4  4.97-4  9.94-4
2.75-2 1.375-2 3.534-2
3.38195e-3 4.12667e-3 3.09830e-2 1.19379e-2
```

```
t
33## f1.0 t
35** 2i 0.0 2i 7.14 2i 7.5 2i 8.0 2i 8.5 2i 9.5 2i 10.5 2i 11.5
     2i 12.0 2i 12.6 2i 15.15 2i 15.5 2i 16.0 2i 16.5 2i 17.5
     2i 18.5 2i 19.5 2i 20.0 2i 20.5 2i 21.0
     4i22.1037 22.58 23.0664 23.5426 8i24.15
     20i33.0 6i54.0 54.635
36$$ 3r1 3r2 3r3 3r4 3r5 3r6 3r7 3r8 3r9 3r10 3r11 3r12 3r13 3r14
     3r15 3r16 3r17 3r18 3r19 3r20 5r21 22 23 24 9r25 21r26 7r27
39$$ 25i1 27
49$$
92235 92238
50$$
18 18
51$$ 7r1 2 3 2r4 5 6 7 2r8 8r9 14r10 6r11 10r12 13 7r14 11r15 12r16
     30r17 16r18 2r19 6r20 3r21 6r22 14r23 27r24 10r25 5r26 27 28 29
     2r30 31 32 33 2r34 2r35 3r36 2r37 38 39 40 41 42 3r43 9r44 t
end
=couple

0$$ a3 3 22 e
1$$ a12 631510 a17 18 17 9 e t
done
end
=origens
0$$ a4 32 a11 86 e
1$$ 1
t
Irradition of Eu portion of control element
3$$ 32 a3 1 a16 2 e
5$$ 2
t
35$$ 0
4t
56$$ 12 12 1 1 a13 1 4 2 a18 1 e
5t
1 gram of Eu
59** f 1.50e12
60** 1 2 4 8 16 32 64 128 256 571.94 1024 1176
66$$ 0 0 0 2 f 0.0
73$$
631510
74**
1.0
75$$ f4
t
56$$ 0 1 a10 12 e
t
60** 0.001
65$$ f0 a5 1 a8 1 a11 1 a14 1 e
t
56$$ f0 t
end
```

Appendix B. DETAILED MODEL OF REGULATING/SAFETY ELEMENT REGIONS WITH ATOM DENSITIES

In the computer model described in Appendix A of ref. 2, the control plate, fuel element side wall, and surrounding water are homogenized to a single zone. Likewise, the safety element, associated water, and aluminum liner for the inner, beryllium reflector are homogenized to a single zone. This is an acceptable practice if the nuclear data are properly processed. However, it is not possible to have a single set of cross sections for a homogenized region that is applicable to all axial locations. During the fuel cycle, the elements are partially withdrawn (see Figs. 3 and 4), leading to the existence of geometries that require a two-dimensional representation for processing of cross section data—an option not currently available in the SCALE package. The deficiency is important when a goal is to calculate the local power density at a location close to the control/safety elements.

The deficiency in cross section processing methods can be mitigated, somewhat, by explicitly representing each material zone in the region between the outer fuel element and the inner, beryllium reflector. These zones are shown in Fig. B.1, and the radii corresponding to the locations noted in the figure are provided in Table B.1. Each control element is composed of 3/16-in.-thick poison

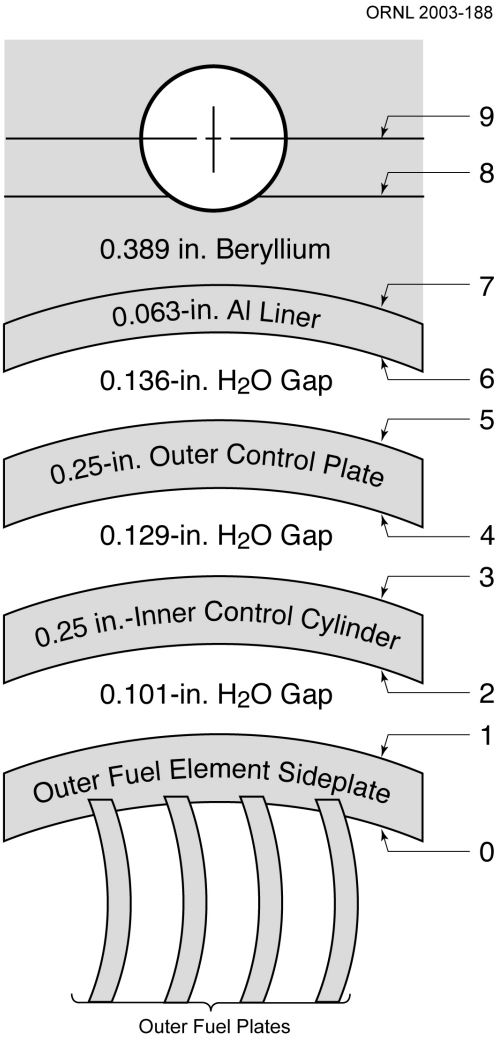

Fig. B.1. Control region configuration.

Table B.1. Geometric configuration of Fig. B.1

Radial location (Fig. B.1)	Distance from core centerline (cm)
0	21.0
1	21.768
2	22.024
3	22.659
4	22.987
5	23.622
6	23.967
7	24.127
8	25.116
9	27.305

(or aluminum) clad with one 1/32-in. aluminum on each side. Physical characteristics of the control and safety elements are provided in Table B.2.

The data in Table B.2 are reported on a "per quadrant" basis. The control element is formed by welding four quadrants. Each safety plate is a single quadrant. The tantalum loading in the control element is reduced by 218 g due to 1/4-in. holes drilled in the gray section of the element (total tantalum loading of 4950 g). Likewise, the total tantalum content of four safety elements, taken together, is reduced by the same amount (combined tantalum loading of 4970 g).

Atom densities for various regions were calculated from these data and are reported in Table B.3. These atom densities were included in the dataset shown in Appendix A.

Table B.2. Summary of pertinent design data for HFIR control plate compacts

Characteristic	Outer plate		Inner plate	
	Gray section	Black section	Gray section	Black section
Principle neutron absorber				
Element	Ta	Eu	Ta	Eu
Specified quantity, g	1297	1922	1292	1912
Chemical form	Ta	Eu_2O_3	Ta	Eu_2O_3
Typical assay, wt %	99.8	86.3	99.8	86.3
Toluene density, g/cm^3	16.46	7.933	16.46	7.933
Rolled core				
Typical dispersion composition, wt %	Al plus 80.64% Ta	Al plus 59.14% Eu_2O_3	Al plus 0.64% Ta	Al plus 59.14% Eu_2O_3
Design total volume, cm^3	206.7	914.3	206.1	909.4
Number of individual compacts	9	18	9	18
Densification of dispersions, % T.D.				
Pressed condition	89	92	89	92
Degassed condition	89	91.5	89	91.5
Rolled condition	94	93	94	93
Typical charged weight of dispersion, g				
Dispersion of Ta or Eu_2O_3	144.44	123.73	143.89	123.06
Matrix aluminum	34.67	85.50	35.55	85.00
Total	179.11	209.23	178.44	208.06
Design compact thickness, in.				
Pressed condition	0.5285	0.5260	0.5240	0.5220
Degassed condition	0.5285	0.5280	0.5240	0.5240

Table B.3. Derived atom densities for control regions (38% tantalum)

Region description	Element	Atom density (atoms per bn*cm)
Outer side plate of fuel + water + inner clad of control element	Al	$4.6012(10^{-2})$
	H	$1.5801(10^{-2})$
	O	$7.9006(10^{-3})$
Control element—europium portion	^{151}Eu	$3.9039(10^{-3})$
	^{153}Eu	$4.2041(10^{-3})$
	O	$1.2162(10^{-2})$
	Al	$3.1562(10^{-2})$
Control element—tantalum portion	Ta	$1.9395(10^{-2})$
	Al	$3.1226(10^{-2})$
Control element—aluminum portion	Al	$6.0307(10^{-2})$
Outer clad of inner element + water gap + clad of outer element	Al	$1.9689(10^{-2})$
	H	$4.4897(10^{-2})$
	O	$2.2448(10^{-2})$
Safety elements—europium portion	^{151}Eu	$3.7630(10^{-3})$
	^{153}Eu	$4.0524(10^{-3})$
	O	$1.1723(10^{-2})$
	Al	$3.0428(10^{-2})$
Safety elements—tantalum portion	Ta	$1.8671(10^{-2})$
	Al	$3.0069(10^{-2})$
Safety elements—aluminum portion	Al	$6.0307(10^{-2})$
Outer clad of outer element + water gap + liner on inner reflector	Al	$2.4754(10^{-2})$
	H	$3.9298(10^{-2})$
	O	$1.9649(10^{-2})$

Appendix C. STUDIES THAT COULD ENHANCE OPERATION OF HFIR

C.1 REVIEW OF EUROPIUM CROSS SECTION DATA

Studies in Sect. 3 led to the conclusion that the bias between measured and calculated k-effectives might possibly be explained by an overestimation of the absorption cross section of europium. If, in the future, the fuel loading in HFIR elements is modified to allow for an increase in the reactor power and/or an increase in the HFIR cycle length from the current values, the europium data in the cross section library should be reevaluated for accuracy and agreement with the most recently measured cross section data. Improved accuracy in the neutronics calculations will lead to a more economical fuel element design, a more economical control plate design, reduced fuel cycle costs relative to an assembly designed with existing data libraries, and reduced uncertainty in the safety-related margins, which leads to potentially higher operating power and subsequent lower cost for experimenters.

C.2 REDERIVATION OF POWER DISTRIBUTIONS FROM CRITICAL EXPERIMENT

The data presented in Figs. 3, 4, and 5 are actually derived from experimental measurements at positions other than those shown in the figures. Appendix A of ref. 1 (pp. 93–96) shows the actual locations at which foils were irradiated. It is possible that if these data were rigorously reexamined, the large discrepancies between calculated and measured local power densities at the edges of the fuel plates could be resolved. An improved level of agreement between calculation and measurement would aid in the design of advanced HFIR fuel elements engineered to achieve higher reactor power and/or longer cycle length.

C.3 REDERIVATION OF BURNUP-DEPENDENT POWER DISTRIBUTIONS FOR USE IN THERMAL-HYDRAULIC ANALYSES (RELAP COMPUTER PROGRAM)

If the studies in part C.2 are successful, then the newly validated computational methods should be used to generate time-dependent power distributions for use with thermal-hydraulic programs. The methods and data would be consistent with state-of-the-art techniques (rather than the code references in ref. 1 that no longer are available), and the accuracy should be equal to or greater than the distributions reported in ref. 1. Implicit in this task would be a validation of the time-dependent methodology using existing, destructive assay measurements of fuel elements (ref. 2).

C.4 IMPROVEMENTS TO EXISTING SOFTWARE

The version of the DORT program used in these analyses is double precision (REAL*8). D. B. Simpson, retired from ORNL, confirmed that the only version of the DOORS software that “might” be double precision is the version designed to be implemented on a DEC/COMPAQ/HP workstation; the type of computer used for calculations reported in this study (a compiler option—real_size 64-exists but is not a part of the standard installation procedure distributed with DOORS 3.2). Eventually, the DOORS software will be installed on a personal computer (PC) that is property of RRD. Conversion of the PC version of DOORS to double precision should be endorsed and supported by RRD. Accuracy in the calculation of the impact of small perturbations on multiplication factor or power profile—the common use for this program for HFIR—would be significantly enhanced by conversion of the program to double precision. The level of effort should be quite small—a few weeks.

C.5 COMMENTS ON ALTERNATIVE COMPUTATIONAL METHODOLOGIES

Analysts familiar with nuclear methods might question if the Monte Carlo theory code, MCNP, should have been used for the analyses described in this report. While it is generally conceded that the computation of multiple, local parameters—in this case, local power densities—is better performed with deterministic methods due to the inherent uncertainty associated with stochastic methods, a perturbation method is available in MCNP to calculate the reactivity worth of small changes in a system (such as differential rod worth and tantalum reduction). Yasunobu Nagaya, Department of Nuclear Energy System, Japan Atomic Energy Research Institute, and Forrest B. Brown, Diagnostics Applications Group, Applied Physics Division, Los Alamos National Laboratory, provided commentary in a presentation at the American Nuclear Society Mathematics and Computations 2003 Topical Meeting,

> "The Monte Carlo perturbation method based on the differential operator sampling method has been widely used to obtain a small change in neutronic parameters or sensitivity. The method is very effective for fixed-source problems but a difficulty arises for eigenvalue problems because the fission source distribution is perturbed. Most Monte Carlo codes assume that the source distribution is unchanged after a perturbation is introduced. However, this assumption can lead to a significant error in the perturbation estimate.
>
> Recently, a method to estimate the perturbed fission source effect has been proposed. In this method, the additional weights for the differential coefficient of the fission source at fission sites are normalized in each cycle, and the effect is estimated by propagating the normalized additional weight between cycles. The method has been implemented into MCNP5 and verified with simple benchmark problems including homogeneous and localized perturbation cases. The conventional MCNP perturbation estimates are significantly improved by taking into account the effect estimated with the method in all the cases. The method is, thus, effective not only for a homogeneous perturbation case but also a localized perturbation case."

At the time these studies were initiated, MCNP5 had not been released for use outside of Los Alamos. HFIR staff should be aware of developments with MCNP in anticipation that improvements in the software will continue to be made. The current state-of-the-art would seem to be that either deterministic or stochastic methods could be used for the solution of problems such as those considered in this report.

Relating to Sect. C.3, if new, cycle-time-dependent power distributions are to be generated, then the computational system must include depletion capability. Depletion cases were not investigated in the studies reported here and, instead, were simulated by various "fresh" critical configurations having boron added to the moderator. The results from using existing ORNL methods for depletion are documented in ref. 3.

ORNL discrete ordinates transport methods (the programs used in the studies documented in this report) do not possess depletion capability. Some investigation is currently being performed on other publicly available packages. Migration to this or similar software should be considered as an option and evaluated prior to initiating future design studies such as increasing reactor power, cycle length, or studying alternative fuels. There is also the potential for increasing the speed and accuracy of the "deep penetration" class of shielding problems and for studies of the transport of particles in beam tubes.

C.6 REFERENCES

1. R. D. Cheverton and T. M. Sims, *HFIR Core Nuclear Design*, ORNL-4621, Oak Ridge National Laboratory, July 1971.

2. A. E. Richt, R. W. Knight, and G. M. Adamson, Jr., *Postirradiation Examination and Evaluation of the Performance of HFIR Fuel Elements*, ORNL-4714, December 1971.

3. R. T. Primm III, *Reactor Physics Input to the Safety Analysis Report for the High Flux Isotope Reactor*, ORNL/TM-11956, Oak Ridge National Laboratory, March 1992.

Appendix D. COMMENTS CONCERNING THE PROCEDURE FOR DETERMINING THE BEGINNING OF CYCLE ESCCEP OF HFIR CONTROL PLATES

Since approximately 1992, data derived from Fig. D.1 have been used to determine an acceptable variance in predicting the symmetric startup position for the control and safety elements for the HFIR. This drawing is excerpted from ref. 1.

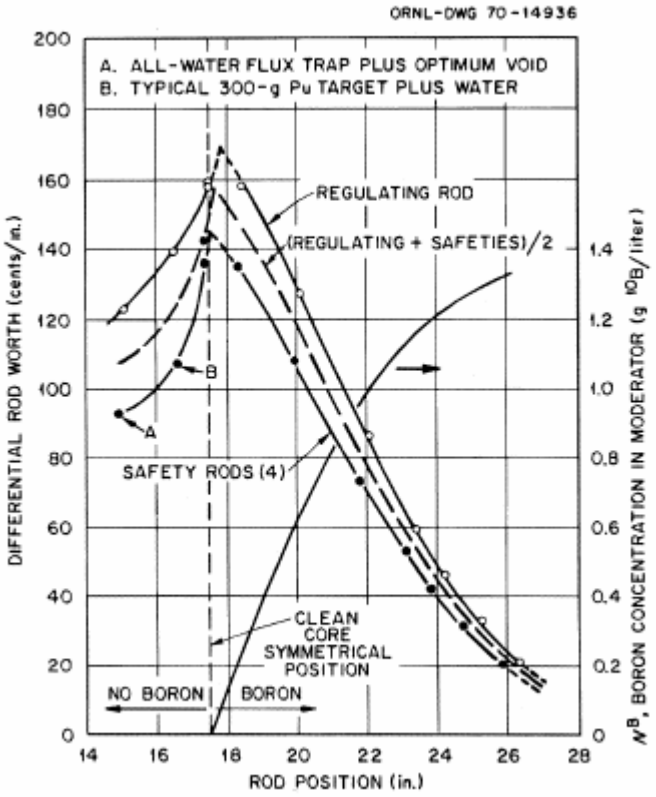

Fig. D.1. Differential worth curves from RRD procedure RTP-2.

Table 9 and Fig. 16 are derived by integrating the differential data presented in Fig. D.1. The curve labeled “safety rods” in Fig. D.1 is derived from differential data presented in Fig. D.2, also from ref. 1 (Appendix A of that reference). As noted in the legend to Fig. D.2, data for safety rod positions less than 16 in. are from critical configurations in which the control element was set at 17.23 in. withdrawn, corresponding to the europium/tantalum interface being located at 5.23 in. below the midplane of the core. (Because of instrumentation differences, the abscissa of Fig. D.2 is off-set 2 in. from Fig. D.1, that is, 25 in. on Fig. D.2 corresponds to 27 in. on Fig. D.1 and likewise, the 15.23 value in Fig. D.2 equates to 17.23 in Fig. D.1.)

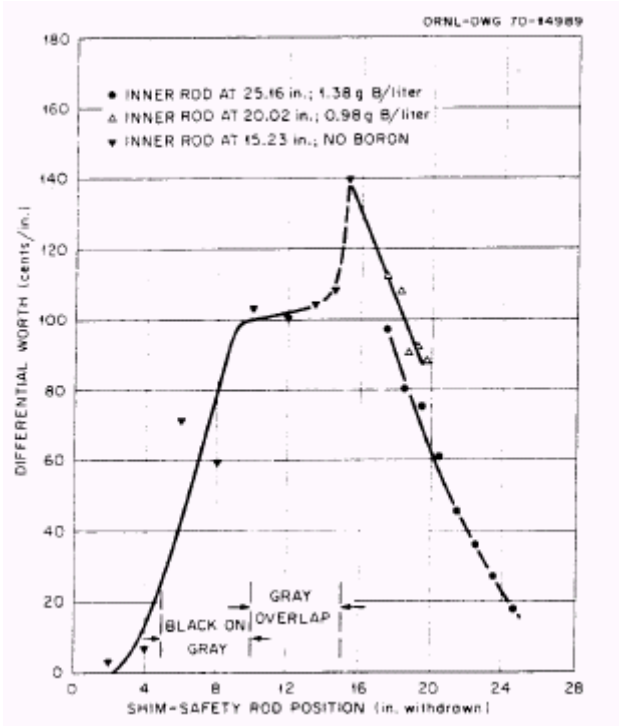

Fig. D.2. Differential rod worth for Eu_2O_3-Ta-Al safety rods in HFIRCE-3 with target.

At 17.23 in. withdrawn, the tantalum-aluminum interface of the control element is almost exactly aligned with the tantalum-aluminum interface of the safety element (interfaces are at –0.23 and +0.23 in., respectively). Figure D.2 (and consequently D.1) indicate an immediate loss of differential worth once the safety plates are inserted to the point that the tantalum regions overlap. Such a prompt drop in differential worth over such a short distance is counterintuitive. Furthermore, given that the reactor is presumed critical at the location in Fig. D.2 corresponding to the highest differential worth (shim-safety rod position of about 15.23 in Fig. D.2), all measurements of differential worth for shim-safety rod positions less that 15.23 in. (if done at critical configurations) were likely performed by "bumping" a single safety plate and extrapolating the measurement to four plates. These measurements would, therefore, be subject to larger uncertainty than measuring small period changes about critical configurations as would have been done for the other data points shown on Fig. D.2.

In ref. 1, the caption for Fig. D.1 states that, except as noted on the figure, these differential curves were obtained from configurations in which boron was present in the moderator and the target region was filled with water. Such conditions do not correspond to currently permitted HFIR operation. Point A on Fig. D.1 is for a configuration with an "all-water flux trap plus optimum void," also not corresponding to HFIR operation. If the worth of the control and safety elements is driven by absorption of neutrons returning from the beryllium reflector, then these differences, perhaps, are only minor perturbations.

Given that the measurements in Fig. D.2 for safety plates appear to coincide with Fig. D.1, it is questionable that the configurations at positions less than 16.6 in. in Fig. D.1 are for symmetric configurations. Calculations presented in this report and symmetric rod worth positions shown in Fig. 9 call into question the advisability of using Fig. D.1 for configurations less than or equal to 17 in. withdrawn. Use of values from Fig. 9 would yield tighter tolerances for predicting startup configurations. Such conservatism seems advisable until such time as new physics measurements are made upon installation of the reduced-tantalum control and safety elements.

Values from Fig. 9 of the combined symmetric differential worth of safety and regulating elements are shown in Table D.1. Also shown are derived values for reduced tantalum elements. These values were obtained by assuming that all critical configurations for reduced tantalum elements were at rod positions 0.3 in. less withdrawn and making use of linear extrapolation to closest integral inch withdrawn value.

Table D.1. Differential worth of control elements at estimated symmetric critical control element positions (ESCCEP)

ESCCEP (inches withdrawn)	Differential rod worth ($/inch)	
	Reference tantalum content (38 wt % Ta)	Reduced tantalum content (30 wt % Ta)
15.0	3.33	3.29
16.0	3.19	3.14
17.0	3.03	2.97
18.0	2.82	2.76
19.0	2.61	2.53
20.0	2.34	2.27
21.0	2.10	2.02
22.0	1.84	1.75
23.0	1.54	1.45
24.0	1.24	1.15
25.0	0.94	0.87
26.0	0.70	0.62
27.0	0.44	0.36

D.1 REFERENCE

1. R. D. Cheverton and T. M. Sims, *HFIR Core Nuclear Design*, ORNL-4621, Oak Ridge National Laboratory, July 1971.

Appendix E. VALIDATION STUDIES APPLICABLE TO THE CALCULATION OF ISOTOPICS IN IRRADIATED CONTROL PLATES

Other than for fresh fuel, no data exist on the isotopics of the material in the tantalum region of the control/safety elements. Reference 1 provides one measurement that can be used for validation. That reference notes that after destructive evaluation of control elements irradiated to 48,615 MWd, "(m)ass spectrographic analysis of the specimen from the tantalum-bearing section of the cylinder indicated that 0.7 neutrons had been absorbed for every tantalum atom initially present."

A SCALE/AMPX/ORIGEN dataset was created to study the depletion of the tantalum region to the specified burnup. This dataset was essentially the same as that provided in Appendix A except the ORIGEN portion of the dataset was for tantalum and was calculated at a reduced burnup. The magnitude of the thermal flux (energy < 0.5 eV) in the tantalum region was taken from the DORT calculation for the BOL configuration that is documented in Sect. 3 (volume-averaged flux over the tantalum regions of both the control and safety plates) and had a value of $1.74(10^{14})$ neutrons/(cm^2·s) for 85 MW. The irradiation time was determined by the burnup and power level (actual time would have been shorter and flux higher due to irradiation at 100 MW). The number of neutrons absorbed per tantalum atom initially present was estimated from the calculated atom densities at 48,615 MWd to be 0.72—excellent agreement with the value determined from measurement. The computation of this parameter requires accurate estimates of the tungsten isotopes as well as ^{182}Ta and ^{183}Ta.

Reference 1 provided isotopic data for the europium region of the control element. These data are presented in Table E.1. Additional SCALE/AMPX/ORIGEN datasets were prepared to calculate the gadolinium content and europium isotopics present at a location 0.5 in. from the Eu/Ta interface. The thermal flux (energy <0.5 eV) at the centerline of the europium region, 0.5 in. from the Eu/Ta interface was taken from the DORT calculation for the BOL configuration that is documented in Sect. 3 and had a magnitude of $1.50(10^{12})$ neutrons/(cm^2·s) for 85 MW. Table E.1 shows the calculated europium/ gadolinium fractions, europium isotopics, and "neutrons absorbed per initial Eu atom." Also shown in Table E.1 are two parametric studies in which the thermal flux was varied to first match the measured "neutrons absorbed per initial Eu atom" and then varied to match the measured Eu/Gd fraction. No information regarding the size of the sample analyzed is known. The variation in flux to match measured quantities is within the spatial variation that occurs, radially and axially, across small distances in the control elements. Nevertheless, these variations in flux do not explain the differences among measured and calculated isotopics. While academically interesting and possibly justification for reviewing the europium cross section data, the studies in this document are concerned with perturbations to the tantalum region of the control and safety plates. The europium regions of those plates will remain unchanged.

Though calculation-to-experiment agreement shown in Table E.1 is poor, experience at the reactor has shown that the worth of the europium region is generally independent of burnup. This is because even though the distribution among isotopes and even elements seems not to be well-known, isotopes of both elements are strong absorbers. Furthermore, those portions of the europium that are 2 in. or more from the Eu/Ta interface receive relatively little neutron fluence, and the europium isotopics are essentially unchanged at EOL (ref. 2). Consequently the shutdown margin of the reactor is essentially unaffected by irradiation.

Table E.1. Comparison of calculated-to-measured physics parameters

Parameter		Measured (ref. 1, 0.5 in. from Eu/Ta interface)	Calculated [assumed thermal flux, n/(cm^2·s) at 0.5 in. from Eu/Ta interface]		
			1.50 (10^{12})[a]	5.40 (10^{12})[b]	3.00 (10^{12})[c]
Fraction (wt %)	Eu	86.5	93.4	74.7	86.4
	Gd	13.5	6.6	25.3	13.6
Europium isotopics (at. %)	^{151}Eu	5.20	33.28	12.95	23.07
	^{152}Eu	8.16	8.44	9.91	10.92
	^{153}Eu	66.92	47.85	48.71	47.58
	^{154}Eu	13.77	9.74	25.40	16.85
	^{155}Eu	5.94	0.59	1.87	1.18
Neutrons absorbed per initial europium atom		1.07	0.29	0.998	0.56

[a]Flux from DORT calculation for beginning-of-life configuration.
[b]Flux to yield reported neutrons absorbed per initial europium atom.
[c]Flux that yields measured Gd/Eu ratio.

E.1 REFERENCES

1. R. W. Knight and A. E. Richt, "Evaluation of Absorber Materials Performance in HFIR Control Cylinders," *Nuclear Technology*, **15**, 384–390 (September 1972).

2. R. T. Primm III, *Reactor Physics Input to the Safety Analysis Report for the High Flux Isotope Reactor*, ORNL/TM-11956, Oak Ridge National Laboratory, March 1992.

INTERNAL DISTRIBUTION

1. Shihjung Chang
2. D. H. Cook
3. R. A. Crone
4. R. J. Ellis
5. M. B. Farrar
6. G. F. Flanagan
7. J. D. Freels
8. J. C. Gehin
9. D. E. Mueller
10. D. J. Newland
11. D. L. Pinkston
12–16. R. T. Primm III
17. C. T. Ramsey
18. K. A. Smith
19. H. R. Vogel
20. J. C. Wagner
21. RRD—Document Control Center

EXTERNAL DISTRIBUTION

22. R. D. Cheverton, 2703 West Gallaher Ferry Road, Knoxville, TN 37932
23. W. J. Marshall, 1907 Huntridge Dr., Clifton Park, NY 12065
24. L. F. Miller, Department of Nuclear Engineering, 314 Pasqua Engineering Building, University of Tennessee, Knoxville, TN 37996-2300
25. R. D. Rothrock, 705 Cordova Lane, Lenoir City, TN 37771